

Article

Sustainable and Efficient Structural Systems for Tall Buildings: Exploring Timber and Steel–Timber Hybrids through a Case Study

Fabrizio Ascione, Francesco Esposito , Giacomo Iovane , Diana Faiella , Beatrice Faggiano and Elena Mele  *

Department of Structures for Engineering and Architecture, University of Naples Federico II, 80125 Naples, Italy; fabrizio.ascione@unina.it (F.A.); francesco.esposito@unina.it (F.E.); giacomo iovane@unina.it (G.I.); diana.faiella@unina.it (D.F.); faggiano@unina.it (B.F.)

* Correspondence: elena.mele@unina.it

Abstract: The paper focuses on tall timber buildings. The major aim of this paper is to identify the most sustainable and efficient structural system to increase the height of timber buildings, also considering steel–timber hybrid structures. First of all, a brief review of tall buildings’ evolution is presented to understand why tall timber buildings are considered nowadays and which are the most adopted structural solutions. Then, the case study of the tallest timber building in the world is selected and utilized as an archetype. Once the model has been validated, seven alternative structural systems are considered by varying the horizontal load resisting system and preserving the same member cross-sections as the reference building. The variants are tested and compared in terms of material consumption, vibration characteristics and lateral load response. Using the best structural system, the height of the building is increased, pushing the structures beyond the current limits and identifying the most efficient option. The idea is to preserve the column cross-sections and balance the increase in gravity loads due to the additional floors by replacing the concrete floors with timber counterparts. With the same structural system, equivalent steel–timber hybrid solutions are finally tested and compared in terms of sustainability to timber-only counterparts and to the original project. The results of analyses show that the use of steel elements combined with timber can lead to optimized and sustainable structural solutions.

Keywords: tall timber buildings; tall buildings; structural systems for tall buildings; steel–timber hybrids; sustainability; life cycle assessment; embodied carbon



Citation: Ascione, F.; Esposito, F.; Iovane, G.; Faiella, D.; Faggiano, B.; Mele, E. Sustainable and Efficient Structural Systems for Tall Buildings: Exploring Timber and Steel–Timber Hybrids through a Case Study. *Buildings* **2024**, *14*, 524. <https://doi.org/10.3390/buildings14020524>

Academic Editor: Chuang Feng

Received: 30 December 2023

Revised: 23 January 2024

Accepted: 10 February 2024

Published: 15 February 2024



Copyright: © 2024 by the authors. Licensee MDPI, Basel, Switzerland. This article is an open access article distributed under the terms and conditions of the Creative Commons Attribution (CC BY) license (<https://creativecommons.org/licenses/by/4.0/>).

1. Introduction

Atmospheric carbon levels and global temperature have steadily risen in recent decades. The planet is 1 °C warmer than it was in the pre-industrialization era, and the value of 1.5 °C is considered as a nonreturn point [1]. With global temperature continuously rising due to mankind’s release of carbon dioxide into the atmosphere, Earth’s climate is changing, as testified by the occurrence of frequent extreme weather events [2]. According to the Paris Agreement of 2015, global temperature rise must be kept below 2 °C, with an additional effort required to limit the temperature increase to 1.5 °C above pre-industrial level. For this aim, emissions should be reduced by 45% by 2030 and should reach net zero by 2050. Considering that nearly 40% of the total global energy-related emissions are due to buildings and the construction sector [3], it is evident that the improvement of design in the sustainability direction could have a remarkable impact [1]. On the other hand, another phenomenon that should be accounted for is the increase in the world population who choose to live in cities. The United Nations estimates that by 2050, the urban population will increase by about 2.5 billion people, or 220 thousand people a day [4,5]. Existing towns will develop into mega towns, reaching populations of about 30–50 million people. Therefore, additional real estate is to be realized for accommodating the needed living spaces; over

the next 40 years, 230 billion square meters of new construction will be built worldwide, adding the equivalent of Paris city to the planet every single week [6]. A further aspect to be considered for steering the cities towards sustainable growth is the containment of land consumption, formally set in Europe to zero net land take by 2050 as an explicit target in the “Roadmap to a Resource Efficient Europe” [7] and in the document “The Future Brief: No net land take by 2050?” [8].

Recently, tall buildings have often been proposed to balance the conflicting needs of urban development and limited land consumption [4,9,10] thanks to the maximum exploitation of the land plot utilized for the building construction. From this perspective, tall buildings appear a reasonable and sustainable solution. However, their sustainability as a building type is broadly disputable since the embodied carbon footprint (computed on a unitary basis) is generally much higher than in the case of their low-rise counterparts. As previously stated, a remarkable improvement in terms of sustainability can be achieved by improving design: in this perspective, the use of timber as a structural material for the realization of tall buildings could be strategic thanks to the inherent sustainability of the wood itself. Several studies demonstrate the favorable environmental balance when using timber or timber products compared to steel or concrete [11]. Timber is 100% renewable, energy efficient and environmentally friendly, requiring less energy to be produced than other structural materials. Furthermore, wood stores carbon during life and prevents it from entering the atmosphere thanks to biogenic carbon sequestration; mechanical efficiency is also not to be overlooked, represented by the strength-to-weight ratio, which is very high for timber and even comparable to steel. Finally, today, timber can be considered an engineered material thanks to the development of new types of products such as glued laminated timber (GLT), cross-laminated timber (CLT) and laminated veneer lumber (LVL).

Timber has always been used as a structural material for low-to-medium-rise buildings, industrial sheds and long-span roofs. The application in the field of tall structures is very recent [12,13] and noticeable advancements occurred starting from the new millennium [14], with several tall timber buildings currently proposed, under construction or recently realized. Some examples are listed hereafter: the Mjøstårnet, the tallest timber building in the world, with a total height of 85.40 m; the Treet, with a height of 49 m; the 25 King, with a height of 46.8 m; and the Origine, in Canada, with a height of 40.90 m. The publication of important guidelines since 2013, such as the “Technical Guide for the Design and Construction of Tall Wood Buildings in Canada” [15] or “Use of Timber in Tall Multi-Story Buildings” [16], as well as the interest of important engineering firms (e.g., SOM) in developing research projects and proposing actual applications [17], highlighted the important role that timber could play in tall building design all over the world. The evolution of national codes, too, testifies to the growing know-how that engineers around the world are acquiring on timber structures.

In this framework, the major aim of this paper is to identify sustainable and efficient structural solutions for timber tall buildings; the idea is to question the limits of timber applications, proposing load resisting systems that allow them to reach greater heights than the buildings realized up until now. For this purpose, a case study is selected, namely the above-mentioned Mjøstårnet, and utilized as an archetype; in particular, once implemented and validated, the numerical model of the actual building structure and different structural systems, using braced frames, CLT shear walls or tube configurations, are considered and analyzed for application at increasing heights. While some of these systems have already been considered in other research (e.g., mass-timber core with CLT panels, in Connolly et al. [18]), the braced tube structure has not been used in practice nor considered for research speculations.

However, it should be observed that timber-only buildings, even at 90–100 m of height, require a large amount of material for large member cross-section sizes and more complex structural systems than steel or concrete alternatives. Therefore, hybrid solutions using steel or concrete structural elements combined with timber members are often proposed, both in the design practice and in the research contexts. Angelucci et al. [19], for example,

propose concrete cores and various timber perimeter structures for the design of a 26-storey building. Several hybrid structures are already realized all over the world, such as the Ascent (86.60 m), the Hoho (84 m), the Haunt (73 m), the Tallwood 1 (41.7 m) and the Sara Kulturhus (72.8 m). Considering the growing attention of steel producers to environmental issues and the production techniques developed with electric arc furnaces using scraps [20] and the very high percentage of recycled steel [20], systems combining timber and steel structural elements (appointed as steel–timber hybrids) are a promising solution in terms of both structural efficiency and environmental sustainability.

Therefore, in this paper, after the exploration of timber-only structures, steel–timber hybrids are considered and designed to increase the height of the tall building case study. Material consumption, response parameters and embodied carbon are evaluated for the different solutions to assess and compare the mechanical efficiency, the structural performance and the sustainability of the solutions.

2. Tall Timber Buildings

Wood has broadly spread as a construction material for tall buildings in the last few years, with a large number of timber-only or hybrid buildings realized, under construction or proposed [13,14]. Figure 1 shows the total height of the tallest timber or hybrid buildings erected in the last decade around the world [14].

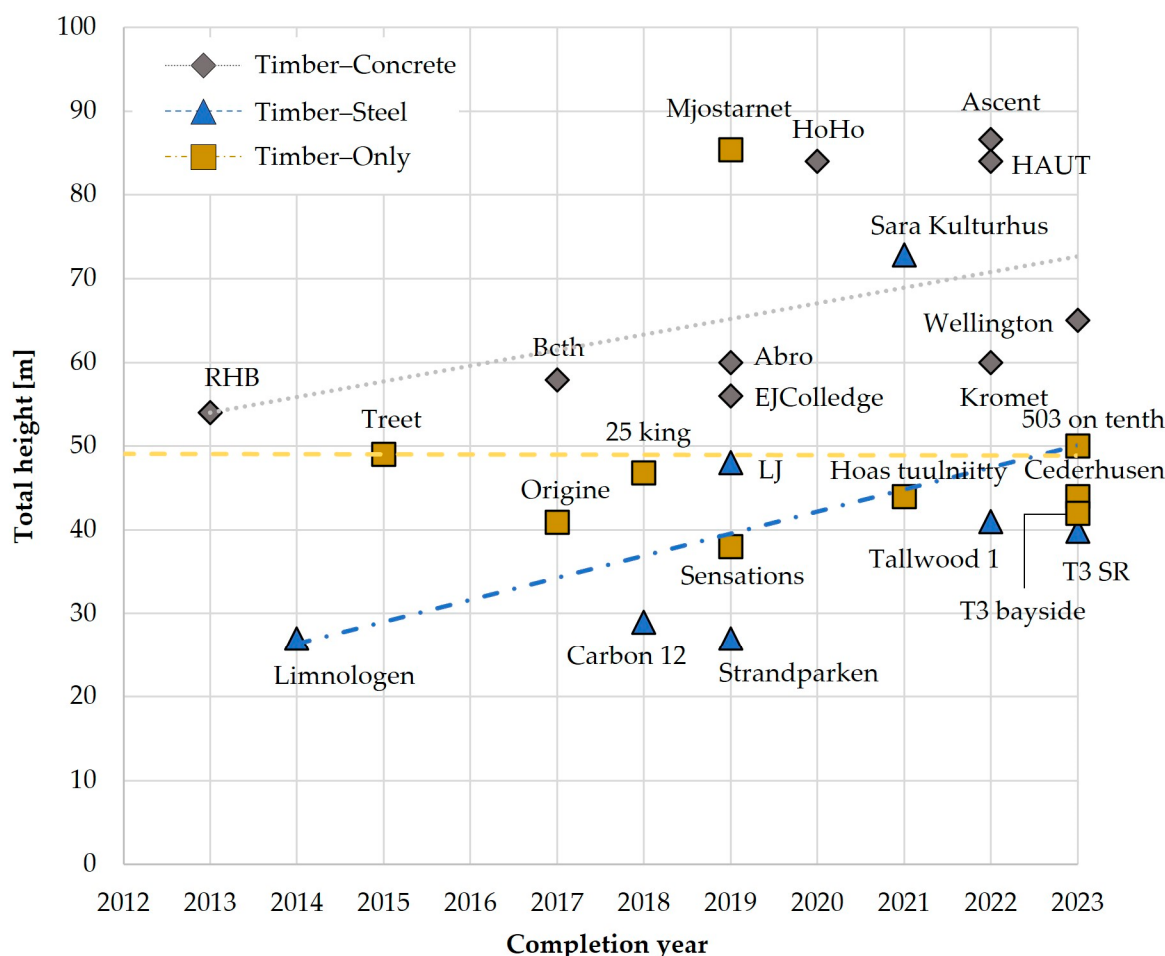


Figure 1. Tallest timber-only, timber–steel and timber–concrete buildings realized in the last decade.

The current design trend is mainly based on the use of reinforced concrete cores or steel braces to give horizontal stability and resistance, while timber elements are only used for vertical loads. However, it can be observed that the tallest timber-only and hybrid

buildings reach more or less the same height, as shown in Figure 2. Further, it is worth noticing that only seven timber buildings are taller than 40 m and only two are taller than 60 m (Figure 3). One of them is the Mjøstårnet, previously mentioned, while the other one is the Pagoda of Fongong, China, realized in 1056 with solid wood. This fact reveals that for almost one thousand years, wood has not been widely adopted as a structural material for high-rise constructions. From 1056 to a few years ago, despite the technological evolution that had led to the birth of numerous industrial timber products, the height of timber buildings had not increased. However, the realization of Mjøstårnet in 2019 [14,21–23], with a height of 85.40 m, shows that, today, the trend is changing.

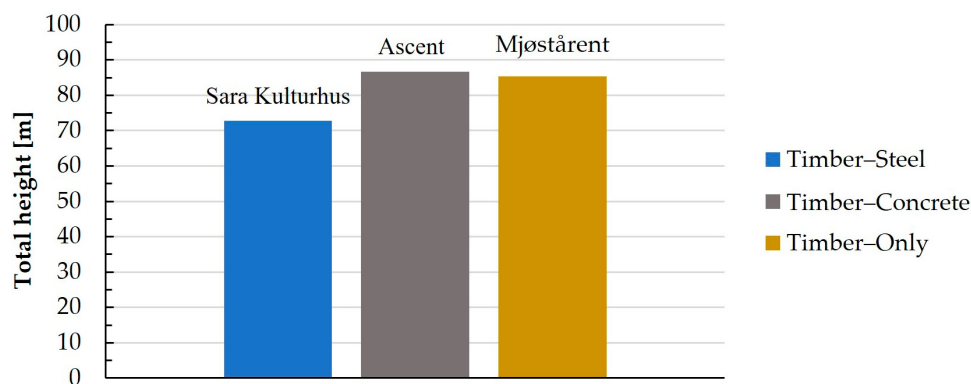


Figure 2. Comparison among the heights of the tallest timber-only and hybrid buildings.

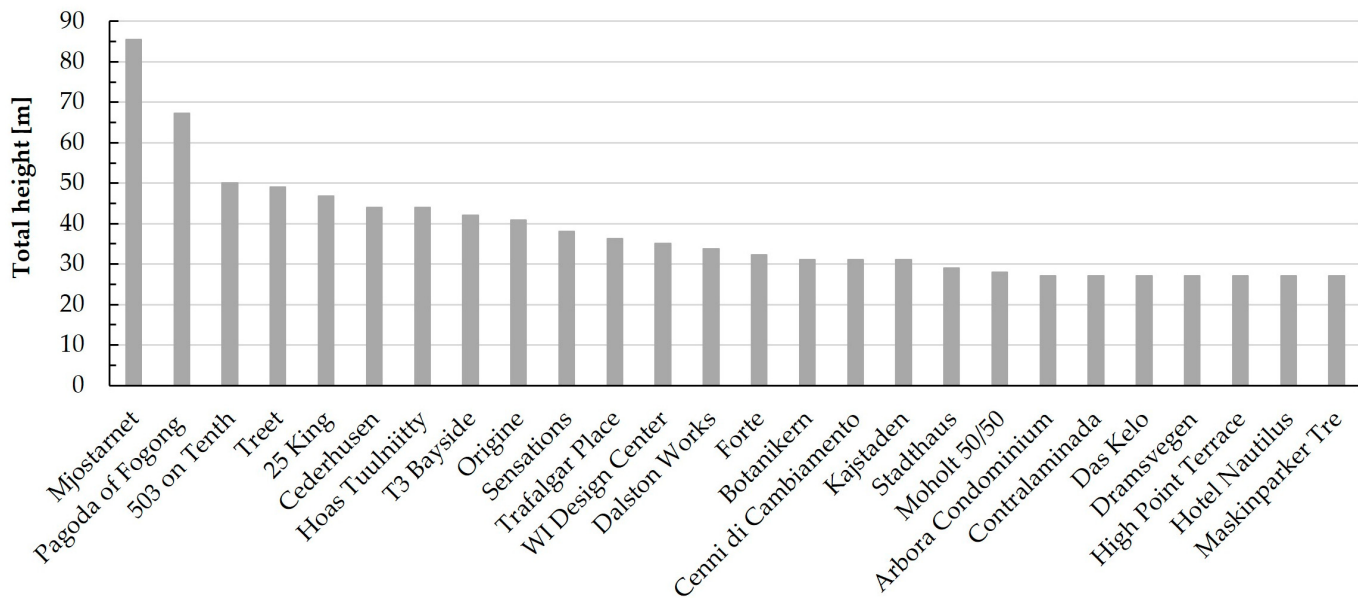


Figure 3. Tallest timber-only buildings in the world.

3. Case Study: Mjøstårnet

3.1. Building Description and Structure Data

The Mjøstårnet is selected as a case study from which several variants are considered. It is the tallest timber building ever built [14]; therefore, studying and analyzing the structural behavior is fundamental to understanding the critical aspects of tall timber building design.

The tower, located in the town of Brumunddal, approximately 140 km north of Oslo, Norway, was designed by the European engineering consultancy company Sweco. According to the Council on Tall Buildings and Urban Habitat (CTBUH) [14], the height to the tip is 88.80 m, while the height to the pergola is 85.4 m, and the height to the highest occupied floor is 68.2 m (Figure 4). The structure has 18 stories, the first five of which are intended

for office use, the next five for a hotel and the remaining ones for residential occupancy. At the top, there is a roof terrace and a restaurant [21].

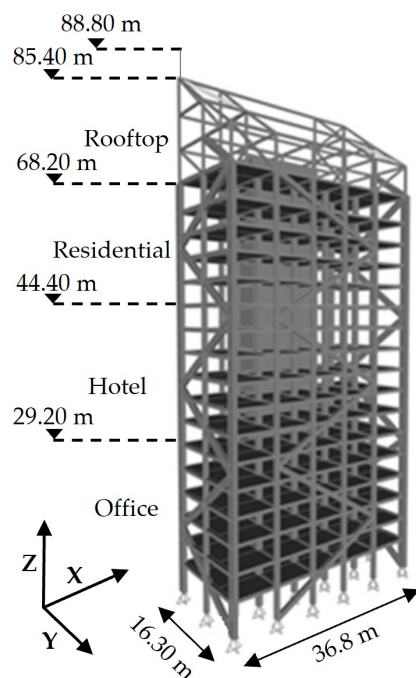


Figure 4. Mjøstårnet building: height and occupancy.

The building has a gravity load resisting system with timber beams and columns. Floors from the 1st to the 11th are prefabricated timber decks based on the Moelven Trä8' system, with a maximum span of 7.50 m [21]. This system is composed of Kerto Q® structural laminated veneer lumber (Kerto-Q LVL) beams, with an LVL bottom and top plate, 36 mm thick acoustic panel and 50 mm thick concrete screed [22]. Stiffening elements, made of Kerto S® structural laminated veneer lumber (Kerto-S LVL), are used in the direction perpendicular to the floor span. From the 12th to the 18th story, 300 mm thick composite concrete floors are used, made of a prefabricated bottom part and a cast-in-place upper part, topped by 50 mm concrete screed and ceramic tiles. As stated by the designers [21,22], the use of concrete for these floors is intended to increase the mass toward the top of the building, thus complying with the comfort criteria for apartments.

The most used cross-sections for interior beams supporting the timber floors are 395×585 and 395×675 mm (Figure 5), while the beam cross-sections supporting the concrete floors are 625×585 and 625×720 mm (Figure 6). The cross-sections of interior columns vary along the height from 810×725 mm to 630×625 mm (Figures 5 and 6).

Large K-diagonals are inserted on the façades to resist the horizontal loads. Cross-sections along the Y and X directions are, respectively, 990×625 mm and 720×625 mm. Perimeter and corner column sections are 625×625 mm and 1485×625 mm, respectively, and both remain constant along the height [21,22]. CLT walls, 200 mm thick, are used in the zones with elevators and staircases, but their contribution to lateral stability has been neglected in the design and analyses [21]. Glulam elements are joined to each other using slotted-in steel plates and dowels, realizing a pinned constraint [21,23].

The wood species used are untreated Norway spruce for the structural members and CU-impregnated Scots pine for the pergola. The glulam grades are GL30h and GL30c, but it is not specified for which element they are used. The CLT strength class is 24 MPa [21–23]. In this paper, GL30h is assumed for columns and braces, GL30c for beams and S355 steel grade for the connections. LVL wood produced by Metsä Wood is used for the floor elements.

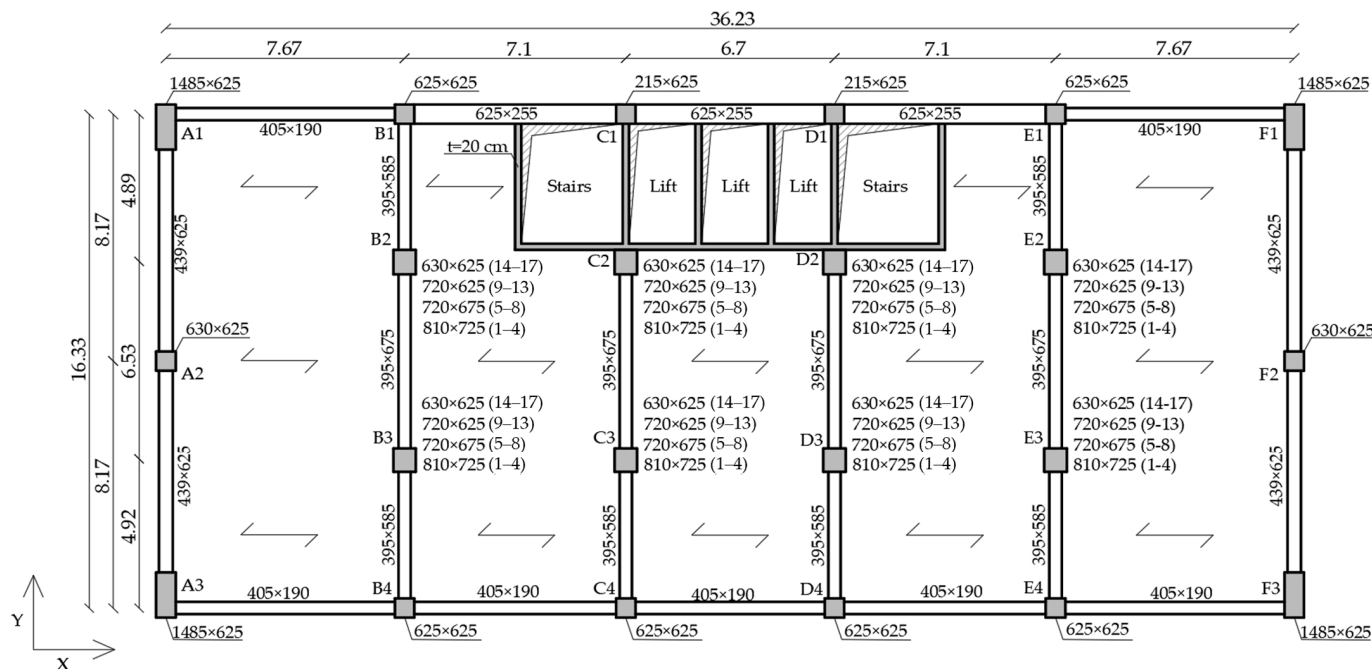


Figure 5. Typical timber floor framing plan.

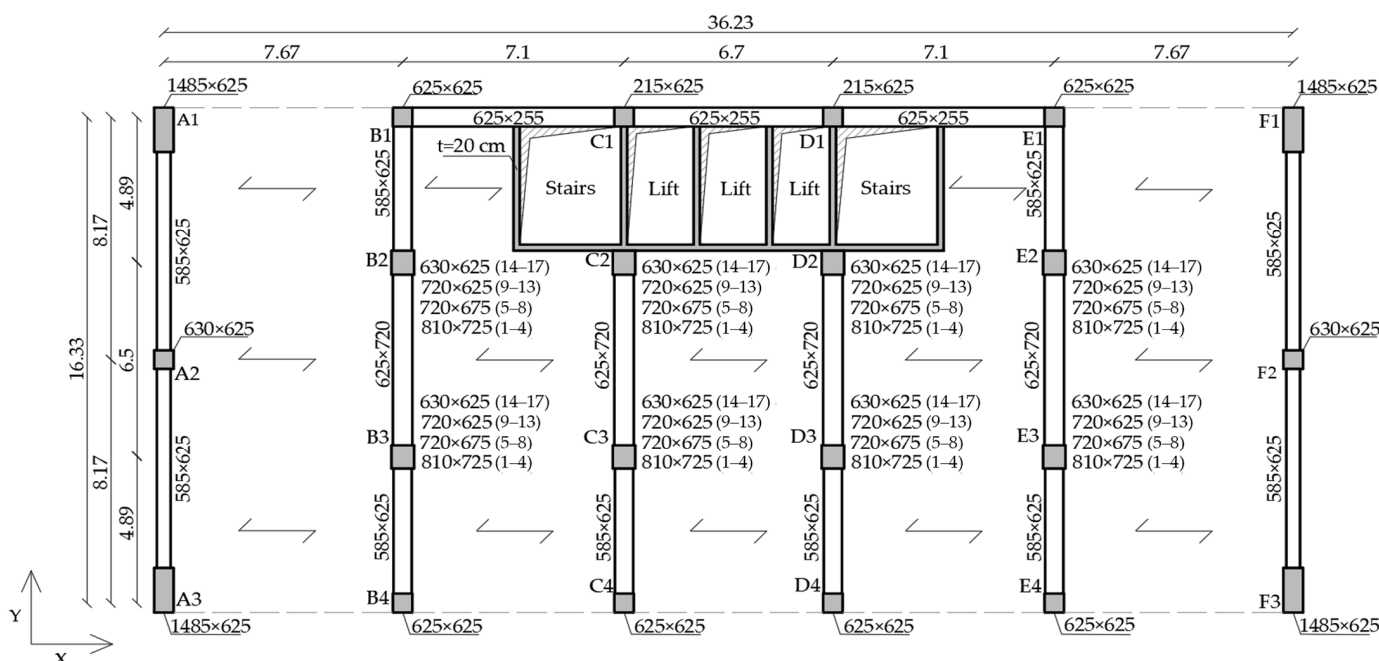


Figure 6. Typical concrete floor framing plan.

Some pictures of the floor structural framing, both timber and concrete, during construction (Figure 7) have been particularly useful in deriving the dead loads. The Metsa timber floor type for levels 1 to 11 (Figure 7c) [24] has a total thickness of 360 mm (for a 7 m span), given by 25 mm of the top flange, 45 mm of the bottom flange and 45 mm of the web element [25]. Knowing this layered configuration, the total weight has been computed and is equal to 1.46 kN/m². The weight of the internal partitions is assumed to be 0.50 kN/m² [23]; the external walls are considered as distributed loads of 1 kN/m² [23]. The total dead load for timber floors is 1.96 kN/m², as also confirmed by data from other sources [26]. Floors 12 to 18 are made of concrete, with a prefabricated bottom part and a

cast-in-place upper part that jointly realize a solid concrete slab (Figure 7b). The floor thickness is 300 mm. Also, in this case, a 5 cm concrete screed and ceramic tiles are considered. The total dead load of the floor is 8.97 kN/m^2 . No information is available on the structural solution used for balcony floors, which are assumed to be made of CLT panels, with a structural weight of 0.50 kN/m^2 [23] and a finishing load of 1 kN/m^2 [23]. Live loads, defined according to Eurocode 1, are shown in Table 1 for the various building occupancies.

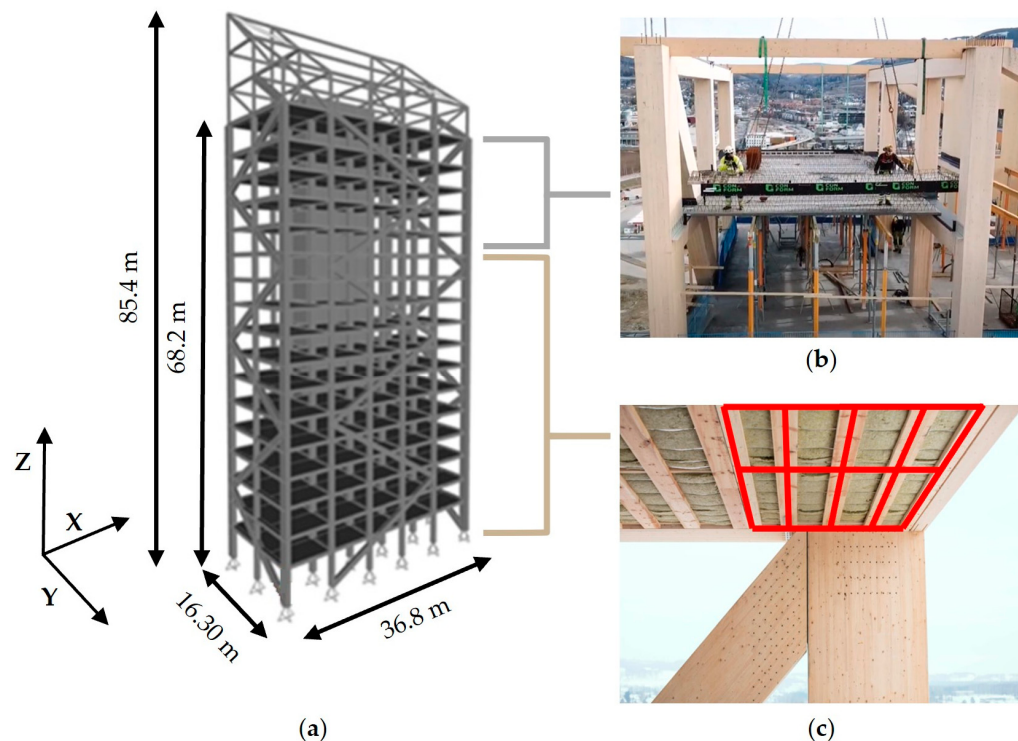


Figure 7. (a) The Mjøstårnet building and floor types; (b) concrete [27]; (c) timber (modified from [28]).

Table 1. Live loads for the various occupancies [23].

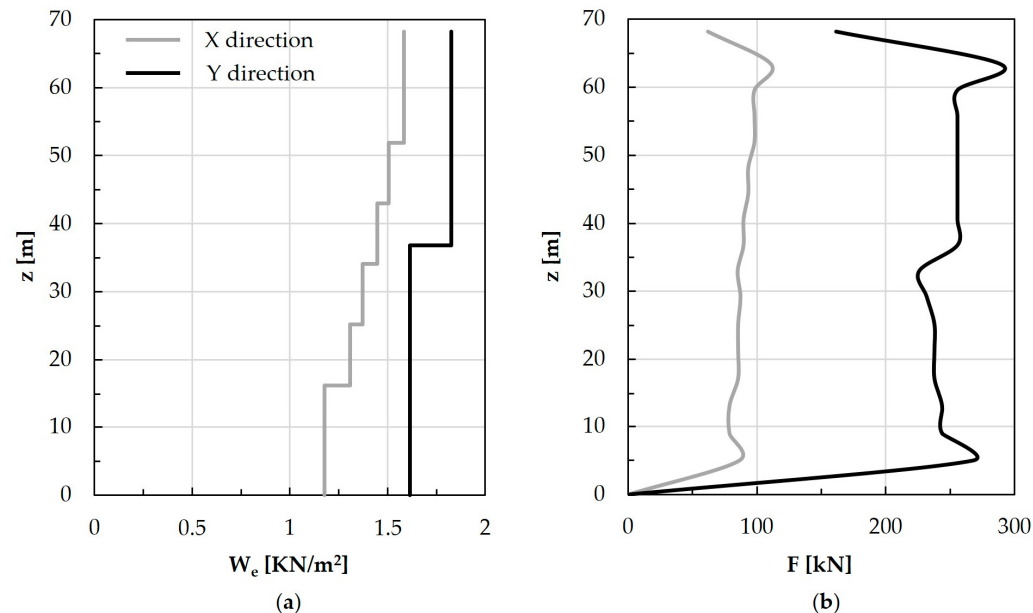
Occupancy	Live Loads [kN/m^2]
Terrace	4.00
Residential	2.00
Hotel	2.00
Office	3.00
Balcony	4.00

Wind action is applied as a static equivalent load, calculated according to Eurocode 1, EN 1991-2002 part 4 and the Norwegian National Annex [21]. The base wind velocity is 22 m/s [21]. The parameters considered for calculations are reported in Table 2; the wind pressures and forces along the height (z) for X and Y directions are, respectively, depicted in Figure 8a,b. The wind forces in the two directions appear very different, though the wind pressures are comparable; quite trivially, this is due to the rectangular plan, which, in turn, determines different areas of the façades under wind pressure. The wind base shear forces are equal to 4163 kN and 1505 kN along the Y and X directions, respectively. Seismic load has not been considered in the design [21,22].

Table 2. Parameters used for wind load calculation (Eurocode 1).

Parameters	
Base wind velocity— v_b	22 m/s
Terrain category	I
Mean wind velocity— $v_m(z)$	32.97 m/s
Turbulence factor— $I_v(z)$	0.11
Exposure factor— $C_e(z)$	4.03
Y— C_p upwind	0.80
Y— C_p downwind	0.70
X— C_p upwind	0.80
X— C_p downwind	0.50

Note: C_p is the pressure coefficient as defined in [29].

**Figure 8.** (a) Wind pressures along X and Y direction; (b) wind forces along X and Y direction.

3.2. FE Modeling and Validation

A FE model of the case study is realized through the structural software SAP2000 v.21 [30]. Beams, columns and diagonals are modeled as unidirectional beam elements; CLT core walls are modeled as bidimensional shell elements; floors are modeled as rigid diaphragms; and all member connections are pinned. Wood is modeled as an orthotropic material; GL30c and GL30h are, respectively, used for timber beams and for timber columns and braces; and CLT is adopted for timber panels. The mechanical properties of GLT (EN 14080:2013 [31]) and CLT (EN 338 [32]) are, respectively, summarized in Tables 3 and 4, including material density (ρ), characteristic bending strength ($f_{m,k}$), characteristic compression and tensile strength parallel to the fiber ($f_{c,0,k}$ and $f_{t,0,k}$), characteristic compression and tensile strength perpendicular to the fiber ($f_{c,90,k}$ and $f_{t,90,k}$), mean modulus of elasticity parallel and perpendicular to the fiber ($E_{0,mean}$ and $E_{90,mean}$) and mean shear modulus of elasticity (G_{mean}). Vertical loads applied to the model include dead and live loads of timber and concrete floors and the load of internal partitions and of external walls, as calculated in Section 3.1. The structural mass is concentrated at the centroid of each floor, where wind forces are also applied (mass and stiffness centroids of each floor are assumed coincident). In order to validate the model, analyses are carried out under the design loads, and the results are compared to those provided by the designers [21,22]. Modal analysis is firstly carried out to check the matching of the building dynamic properties with the values reported by the designers; then, gravity plus wind load combination, defined according

to Eurocode 1, is considered, and the following response parameters are compared: axial force in corner columns, top drift and top floor acceleration.

Table 3. GLT mechanical properties.

	ρ [kg/m ³]	$f_{m,k}$	$f_{c,0,k}$	$f_{c,90,k}$	$f_{t,0,k}$ [MPa]	$f_{t,90,k}$	$E_{0,mean}$	$E_{90,mean}$	G_{mean}
GL30c	430	30.00	25.50	2.50	19.50	0.50	13,000	300	650
GL30h	480	30.00	30.00	2.50	24.00	0.50	13,600	300	650

Table 4. CLT mechanical properties.

	ρ [kg/m ³]	$f_{m,k}$	$f_{c,0,k}$	$f_{c,90,k}$	$f_{t,0,k}$ [MPa]	$f_{t,90,k}$	$E_{0,mean}$	$E_{90,mean}$	G_{mean}
CLT	420	24.00	21.00	2.50	14.00	0.50	6960	300	650

Concerning the vibration periods of the building, the $T_x = 3.03$ s and $T_y = 2.70$ s values given by the designers for the X and Y directions, respectively [33], are considered as a reference (Figure 9a). The comparison with the values obtained for the FE model is reported in Figure 9b and Table 5. The difference between the results obtained here and the original project values is of the order of 10%, which can be considered acceptable.

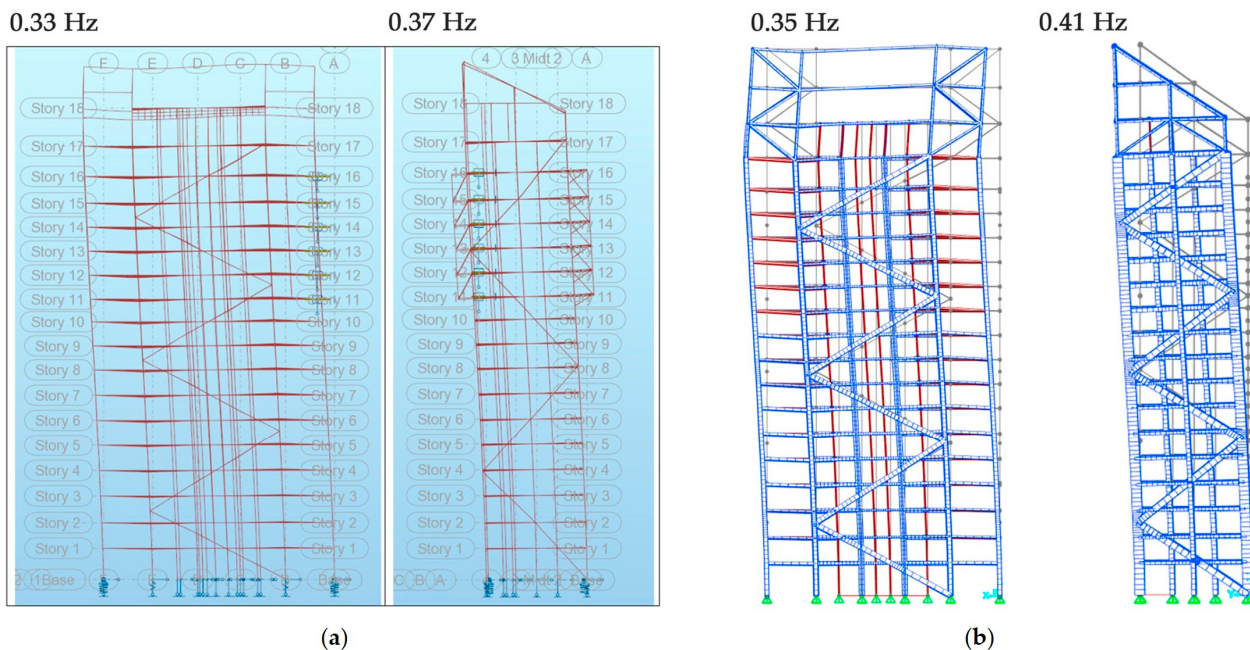


Figure 9. Fundamental vibration periods and modal shapes: (a) designers [33], (b) FE model.

Table 5. Fundamental vibration periods: values from the designers and the FE model.

	Designers	FE Model	Δ [%]
T_x [s]	3.03	2.84	6.2
T_y [s]	2.70	2.42	10

The reference value from the designers for the maximum axial force in the corner columns under gravity and wind is 11,500 kN (compression) [21], while the counterpart obtained from the FE analyses is equal to 11,276 kN; thus, the difference is equal to 2%.

The top displacement given by the designers is 140 mm (also considering the upper pergola) [21]. In the present study, nonlinear static analyses, accounting for P-Delta effects, have been conducted. The results in terms of the horizontal displacements of each story in the X and Y directions are provided in Figure 10a. The top displacement obtained from the FE model is 123 mm, which differs from the value provided by the designers by 12% but is still considered acceptable.

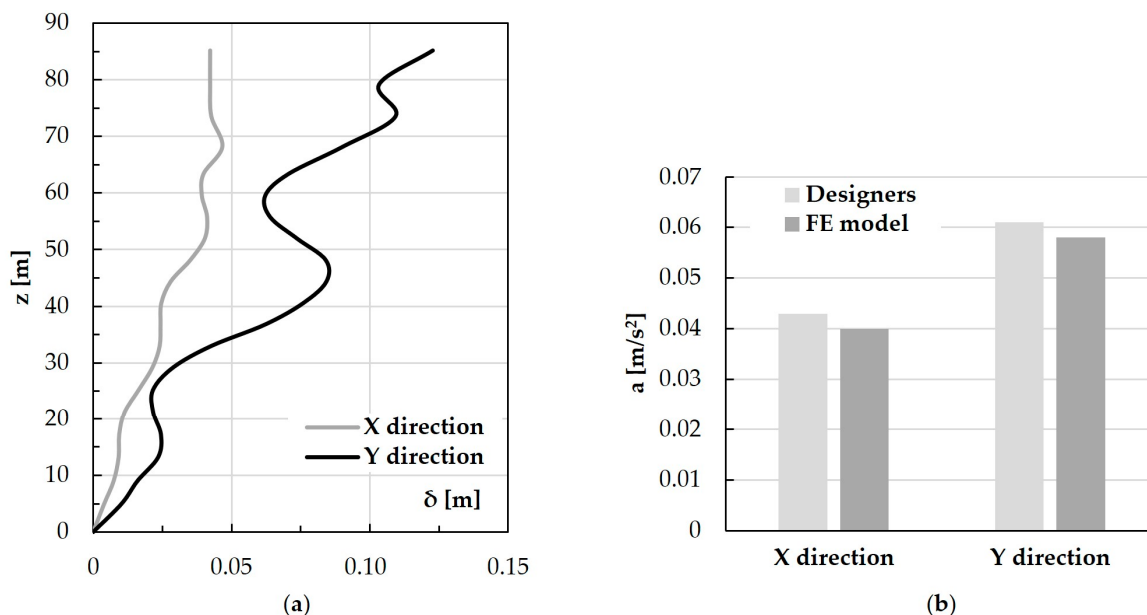


Figure 10. (a) FE model lateral displacements; (b) top floor accelerations: results and comparison.

Finally, the maximum top floor acceleration due to the wind action is evaluated and compared to the reference value provided by the designers (Figure 10b). It is worth recalling that induced vibrations can cause discomfort to the building occupants, thus limiting the functional effectiveness of the structure. In order to account for this further limit state, which is particularly important for tall flexible structures, a simplified procedure is suggested by the codes and standards. To this aim, the standard ISO 10137:2007 [34], which gives recommendations on serviceability against vibrations of buildings, is adopted, as it was by the designers of the Mjøstårnet case study. The top floor acceleration is evaluated according to this procedure through structure and wind action parameters, which were checked against the limit value and compared to the designers' outcome.

The parameters involved in the check procedure are given in Table 6. The procedure consists of (i) calculating the top floor acceleration, according to the formula (1) [34], (ii) setting the representative point of acceleration (A) as a function of the frequency (f_0), as shown in Figure 11, and (iii) contrasting this point against one of the limit curves, depending on the floor's intended occupancy (in this case, residential [21]).

Formula (1) is given by the following:

$$a = \sigma_{a,x}(z) \cdot k_p, \quad (1)$$

where:

- $\sigma_{a,x}(z) = (c_f \cdot \rho \cdot b \cdot I_v(z_s) \cdot v_m(z_s)^2 \cdot m_{1,x}^{-1}) \cdot R \cdot K_x \cdot \phi_{1,x}(z)$ is the standard deviation of the acceleration, where c_f is the force coefficient, ρ is the air density, b is the width of the structure, z_s is the reference height, $I_v(z_s)$ is the turbulence intensity at the height $z = z_s$, $v_m(z_s)$ is the mean wind velocity for $z = z_s$, $m_{1,x}$ is the along wind fundamental equivalent mass, R is the square root of the resonance response, K_x is the nondimensional coefficient and $\phi_{1,x}(z)$ is the fundamental along wind modal shape;

- $k_p = [2 \cdot \ln(\nu T)]^{0.5} + 0.6 \cdot [2 \cdot \ln(\nu \cdot T)]^{-0.5}$ is the peak factor, where ν is the up-crossing frequency and T is the average time for the mean wind velocity.

Table 6. Parameters used for the calculation of top floor acceleration.

Parameters	
Fundamental frequency along X— η_x [Hz]	0.35
Fundamental frequency along Y— η_y [Hz]	0.41
Fundamental equivalent mass— m_i [t]	7106
Reference height— z_s [m]	40.92
Force coefficient— c_f [-]	1.40
Turbulence factor— $I_v(z_s)$ [-]	0.11
Mean wind velocity— $v_m(z_s)$ [m/s]	32.97
Air density— ρ [kg/m ³]	1.25
Modal shape— $\Phi(z)$ [-]	0.36
Peak factor X— $K_{p,x}$ [-]	3.38
Peak factor Y— $K_{p,y}$ [-]	3.36
Structural damping— δ_s	0.06
Aerodynamic damping X— δ_{a1}	0.01
Aerodynamic damping Y— δ_{a2}	0.02
ζ [-]	2.00
K_x [-]	1.75

The results here obtained are very close to the designers' ones, presented in [21], as can be seen in Figure 10b as well as in Table 7, with differences of 6.9% and 4.9%, respectively, along the X and Y directions.

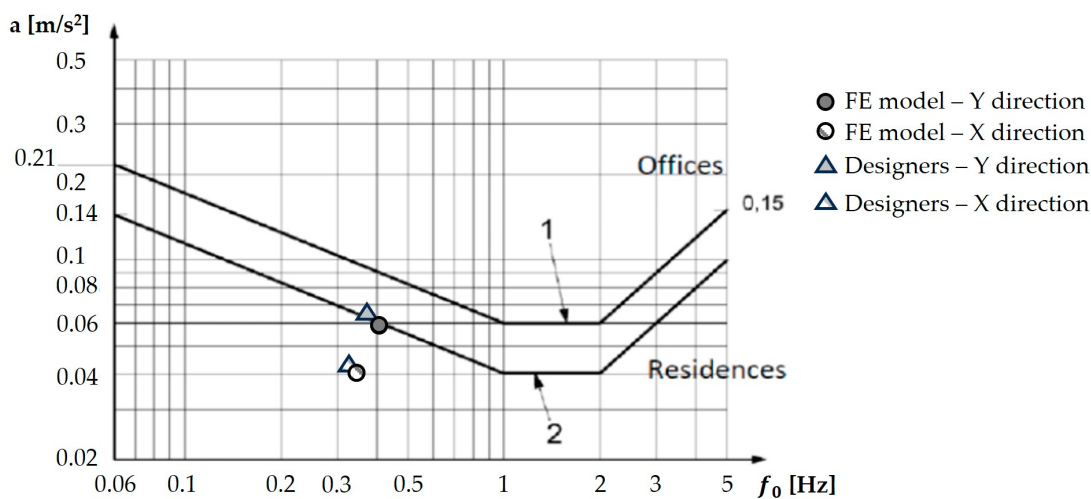


Figure 11. Serviceability check: designers vs. FE model (redraw from [21]).

Table 7. Serviceability analyses results and comparison with reference values.

	Designers	FE model	Δ [%]
a_x [m/s ²]	0.043	0.040	6.9
a_y [m/s ²]	0.061	0.058	4.9

Considering the comparisons made in terms of periods, top drift and acceleration, it can be stated that the differences are always equal to or less than 10–12%. Therefore, the model can be considered validated and it can be used for further analyses.

4. Definition and Assessment of Timber Structural Variants

4.1. Structural Variants Investigated

Alternative lateral load resisting systems are proposed and analyzed in order to establish the most efficient solutions to increase building height. Seven variants of the lateral load resisting system, which preserve the same member cross-sections of the original project, are analyzed and shown in Figure 12.

	Project	K-braces + CLT core	X-braces + CLT core	V-braces + CLT core	Braced tube + CLT core	CLT panels + CLT core	CLT core	R.C. core
CLT core		×	×	×	×	×	×	
R.C. core								×
K- X- V- braces	×	×	×	×	×			
Perimetral CLT Panels						×		

Figure 12. Alternative structural systems.

Changes among variants are also provided in Figure 12 as visual sketches identifying four groups of lateral load resisting systems, namely CLT core, R.C. core, braces (K-, X- and V-shaped) and perimetral CLT panels.

In particular, the CLT core, present in the original project but neglected in the analyses under horizontal loads by the designers, is accounted here for all variants. Five variants are configured as dual core-perimeter structural systems: the first three systems have K (K-braces + CLT core), X (X-braces + CLT core) or V (V-braces + CLT core) timber diagonal bracings superimposed to the perimeter frames and CLT core; the fourth one (braced tube + CLT core) is a braced tube with X diagonal bracings on the four façades, converging at the column corners; the fifth variant adopts CLT panels at the four building corners, working as mega-columns, in addition to the core. Finally, the sixth and seventh solutions adopt a structural core only for the lateral resisting system, made of either CLT panels or reinforced concrete walls. An additional case is also created from the original project system by replacing the concrete floors with timber floors.

For each alternative structural system, an FE model is created considering the structures up to 68.2 m (the highest occupied floor), and the following different analyses are carried out: modal analyses, gravity loads only analyses, gravity plus wind loads analyses and simplified serviceability analyses. From them, the following parameters are evaluated:

- Total structural mass;
- Fundamental vibration characteristics along the X and Y directions;
- Lateral displacements along the X and Y directions, contrasted against the limit of $H/500$;
- Inter-story drift along the X and Y directions, contrasted against the limit of $h/200$ (h is the inter-story height, equal to 4 m);
- Top floor accelerations in both the X and Y directions, according to the relevant building frequencies, contrasted against the limit imposed for residential use at the specific building frequencies along the X and Y directions.

4.2. Structural Analyses

4.2.1. Structural Mass

First, a comparison in terms of total structural mass is reported in Figure 13 with also the percentage variation in mass with respect to the project model. The K-braces + CLT core, X-braces + CLT core and V-braces + CLT core, as well as the braced tube + CLT core, all have almost the same mass as the original model with a variation between 0% and 1.4%. Clearly, using a reinforced concrete core, the structural mass significantly increases (+63%). The case of the original structure without concrete floors (project—all timber floors), also depicted in Figure 13 with a percentage change in mass with respect to the project model equal to −39%, shows that the mass can be significantly reduced using all timber floors, thus opening the possibility to increase the height of the building.

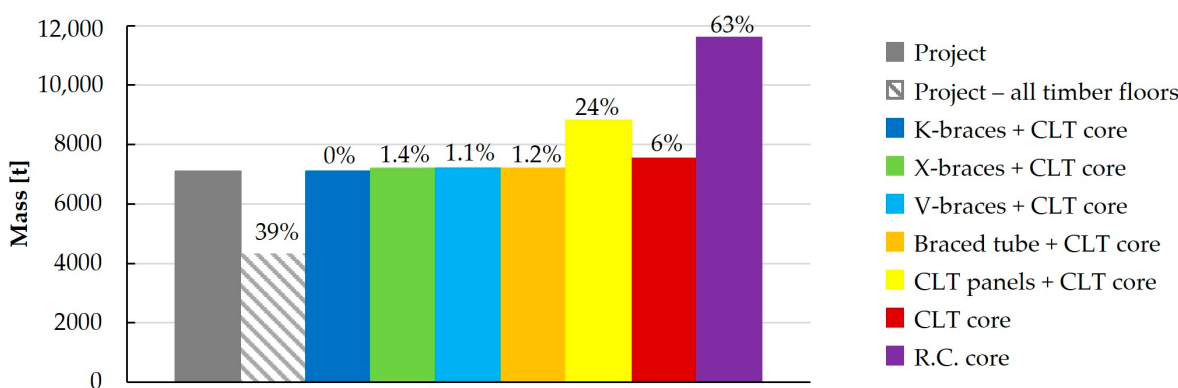


Figure 13. Total structural mass of the original project and the variants.

4.2.2. Vibration Characteristics

The first vibration period calculated for each model along X and Y are reported in Figure 14, together with the variation with respect to the project model. Systems with X-braces + CLT core and V-braces + CLT core have almost the same period values, lower than their K-braces counterpart (9–11%), with a percentage change with respect to the project model between 34 and 36%. The braced tube solution is very rigid, with period values equal to the V-braces along Y and close to the case with a reinforced concrete core along X (3%). The longest period values are obtained in the case of the CLT core only with a value of 2.45 s along X and 4.90 s along Y.

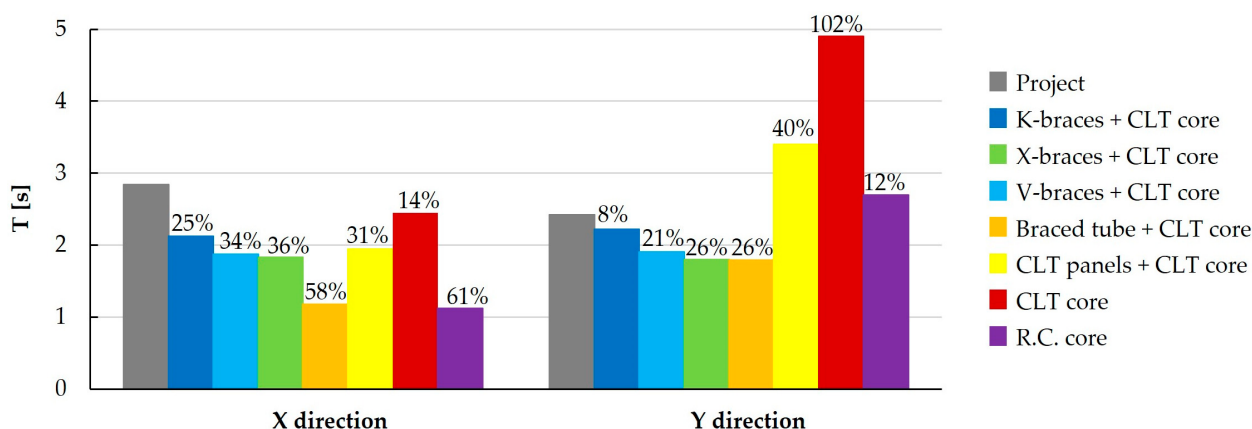


Figure 14. Vibration periods of the original project and the variants.

4.2.3. Lateral Displacements and Inter-Story Drifts

The lateral displacement profiles in the Y direction (the weakest one) are reported in Figure 15. Structural systems with V-braces + CLT core and X-braces + CLT core, as

well as the braced tube + CLT core, perform better than the other variants and the original project. The direct comparison between the structural system of the original project and the one with K-braces + CLT core shows that the top displacement is the same; however, the drifts of the floors within the K-bracing endpoints that characterize the deformed shape of the original project are eliminated thanks to the presence of the CLT core that regularizes the deformation profile by ensuring uniform stiffness along the height. The largest displacements are obtained by the variants with only a CLT core and with CLT panels + CLT core, confirming the results obtained in the modal analysis. In particular, the percentage variations in the top floor lateral displacement of the examined structural variants with respect to the limit of $H/500$ are as follows: -33% for K-braces + CLT core, -26% for R.C. core, -56% for V-braces + CLT core, -48% for X-braces + CLT core, -52% for the braced tube + CLT core and $+43\%$ and $+251\%$, respectively, for the case of CLT panels + CLT core and CLT core only.

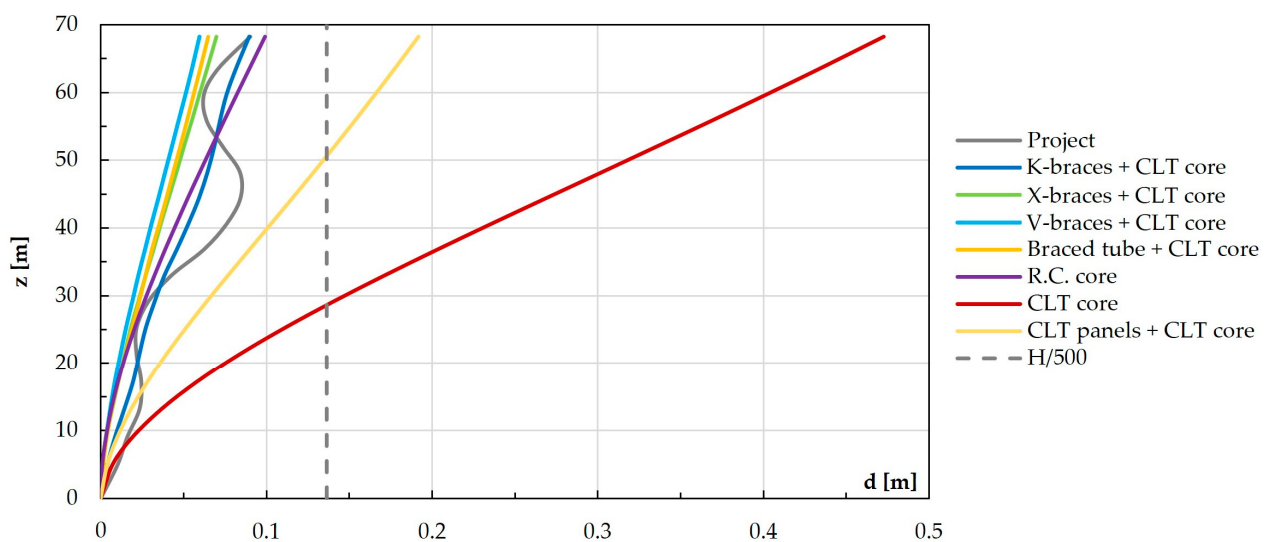


Figure 15. Lateral displacement profiles along Y for the original project and the variants.

Inter-story drifts computed for the original project and the seven variants' models along the Y direction are reported in Figure 16.

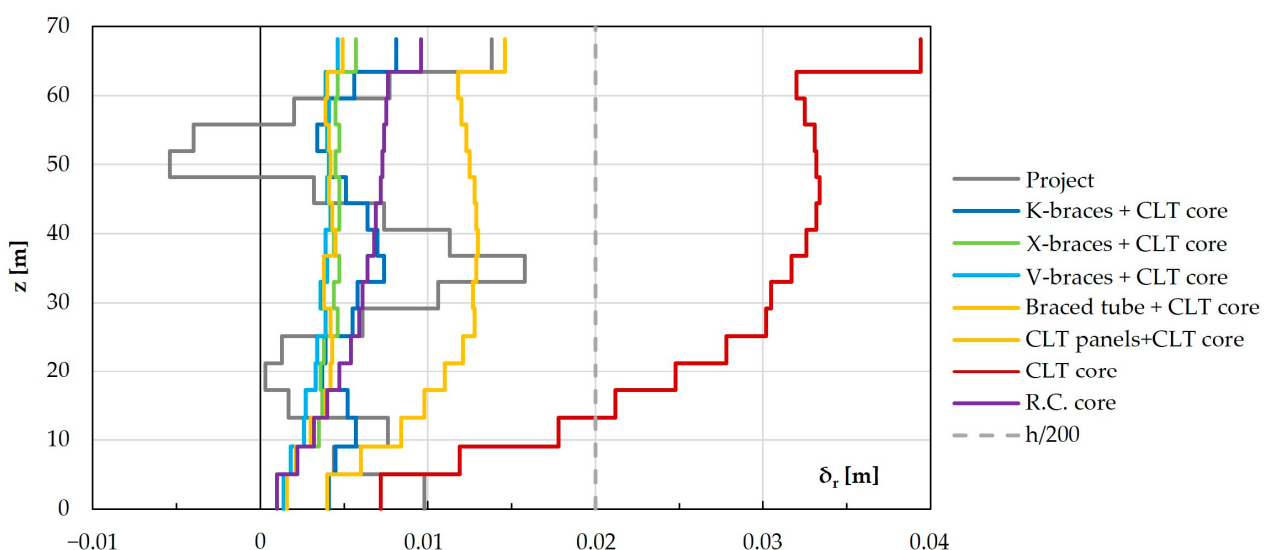


Figure 16. Inter-story drifts along Y for the original project and the variants.

In all cases, except for the CLT core only, the values are lower than the limit of $h/200$, and it can be clearly observed that the presence of the core, either CLT or reinforced concrete, regularizes the deformed shape and reduces the relative drifts. The largest drifts are obtained in the case of the CLT core.

In particular, the percentage variations in the top floor inter-story drift of the examined structural variants with respect to the limit of $H/200$ are as follows: -60% for K-braces + CLT core, -52% for R.C. core, -77% for V-braces + CLT core, -72% for X-braces + CLT core, -76% for the braced tube + CLT core and -27% and $+97\%$, respectively, for the case of CLT panels + CLT core and CLT core only.

4.2.4. Floor Accelerations and Serviceability Checks

A comparison of serviceability analysis and checks is reported in Figure 17 in terms of top floor accelerations, a , both compared with the imposed limit (a_{lim} ; Figure 17a) and as a function of the frequency (f_0 ; Figure 17b). With regard to the serviceability checks, this verification is also critical along the Y direction, where wind action is more severe and the structure is more flexible. Along the X direction, in fact, top floor accelerations are always under the imposed limit; along Y, instead, values are always close to, or even larger than, the limit value. It is important to recall that the limit itself varies according to the frequency, as clearly shown in Figure 17. As already underlined for the displacement analyses, the structural systems with V- and X-braces + CLT core, as well as the braced tube + CLT core, perform better than the other variants and the project model.

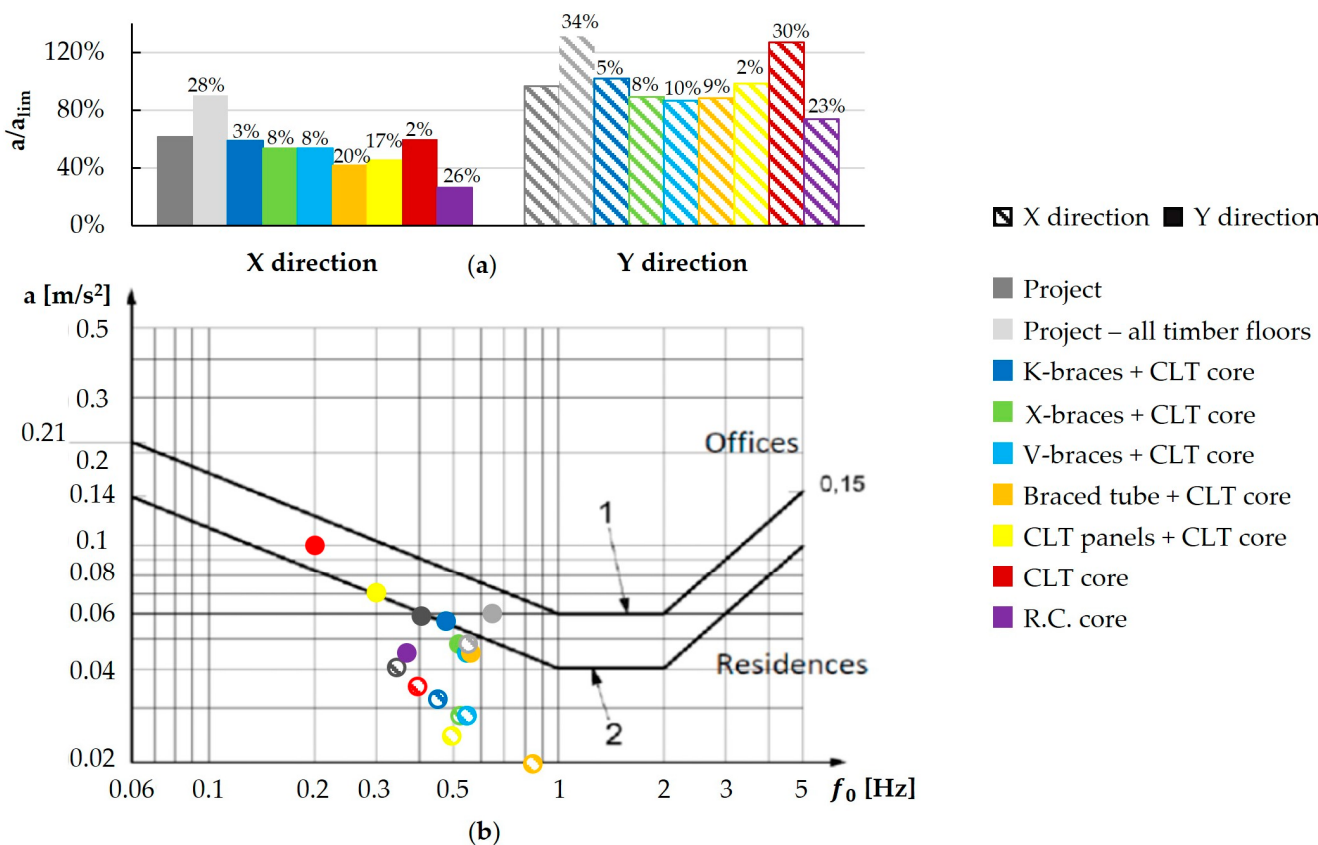


Figure 17. Serviceability analysis results' comparison (redraw from [21]).

In particular, the percentage variations in the top floor accelerations of the structural variants with respect to the original model are as follows: $+28\%$ and $+34\%$ (along the X and Y directions) for the project—all timber floors, -3% and $+5\%$ for the K-braces + CLT core, -8% and -8% for the X-braces + CLT core, -8% and -10% for the V-braces + CLT core, -20% and -9% for the braced tube model, -17% and $+2\%$ for the CLT panels + CLT core,

−2% and +30% for the CLT core and −26% and −23% for the R.C. core. The structure with a reinforced concrete core exhibits the best performance, albeit at the cost of a significant increase in mass.

Figure 17 also shows the case of the original structure without concrete floors (project—all timber floors), with accelerations significantly exceeding the imposed limit. The comparison between the two cases, i.e., the project model and project—all timber floors, clearly explains the reason underlying the introduction of such concrete floors.

5. Exploring Solutions for Increasing Height

5.1. Structural Systems and Preliminary Considerations

For some of the proposed variants, broad margins between capacity and demand values arise from the analyses and checks discussed in the previous section. This observation suggests the possibility of increasing the building height, thus pushing the limit currently reached by timber buildings with the Mjøstårnet case study.

The systems that have shown better performance and lower demand-to-capacity ratios are the braced frames (K-, X- and V-braces) and the braced tube. These structures are here considered to increase the building height as much as possible.

As a first step, a preliminary check should be carried out for the gravity load resisting system of the building to assess the extra capacity necessary for compression to support the load increase deriving from the additional floors. The idea is to preserve the column cross-sections and to balance the replacement of the concrete floors with timber counterparts. Figure 18 shows the compression demand-to-capacity ratio (DCR) of the existing columns with and without concrete floors. Quite trivially, the load reduction due to the difference between the weights of concrete and timber floors ensures a larger margin (lower DCR) to sustain the load increase deriving from additional floors. However, in the previous section, it has been shown that by reducing the floor mass, the floor acceleration increases, making the serviceability check highly critical. Therefore, to increase the building height by exploiting the available margin between the compression capacity and the gravity load demand, further enlarged through the concrete floor substitution, very stiff and efficient structural systems should be used to prevent excessive displacements and accelerations.

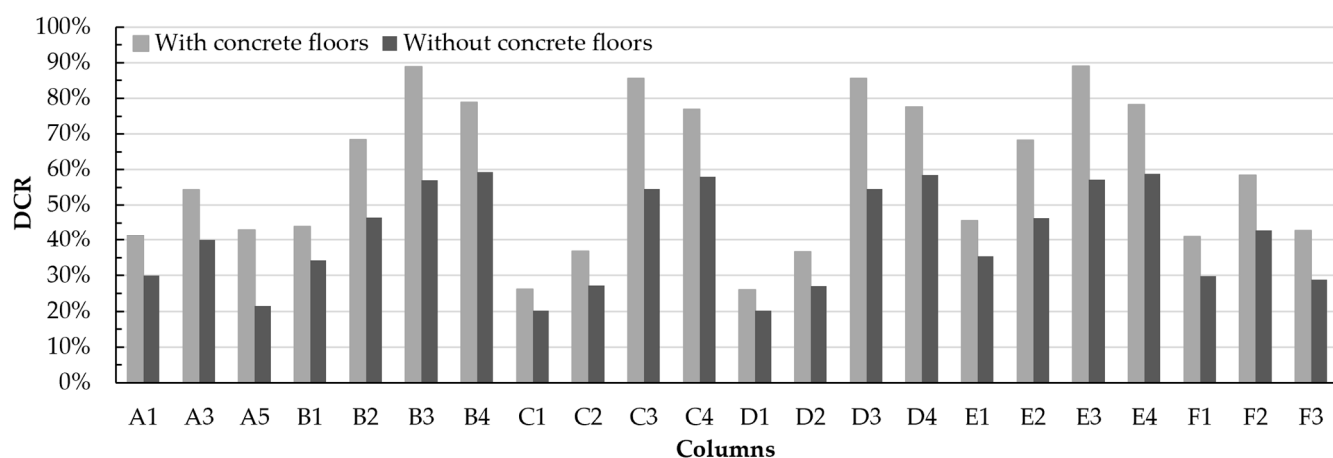


Figure 18. Column compression DCR with and without concrete floors.

5.2. Stepwise Increase in the Building Height

5.2.1. Analyses Performed

The building height has risen through stepwise increments. In particular, the following three steps have been considered (Figure 19):

1. Addition of three floors, height increase $\Delta H = 12$ m, total height reaching 80.20 m;
2. Addition of five floors, height increase $\Delta H = 20$ m, total height reaching 88.20 m;
3. Addition of seven floors, height increase $\Delta H = 28$ m, total height reaching 96.20 m.

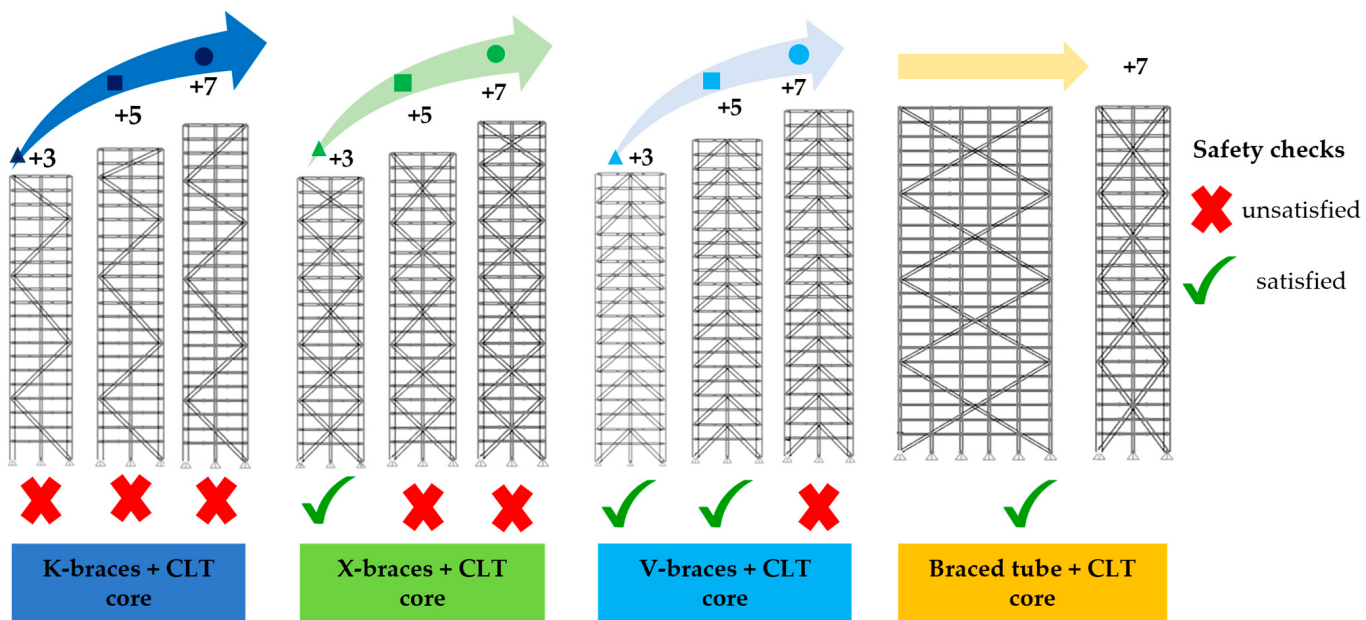


Figure 19. Analyses steps considered to increase the height for the four structural systems studied.

The inter-story height is 4 m, and the occupancy for the additional floors is always residential. For each step, both member checks (strength and stability) and global serviceability checks (in terms of displacements, inter-story drifts and floor accelerations) have been executed to guarantee the feasibility of the proposed solutions. The total structural mass and the fundamental vibration periods have been also derived. Only for the solution with braced tube + CLT core is the last step of the analyses carried out. The base shear for the three steps along the X and Y direction is, respectively, equal to step 1 (+3 floors), 1812 kN and 5014 kN; step 2 (+5 floors), 2047 kN and 5558 kN; and step 3 (+7 floors), 6104 kN and 2276 kN.

From Figure 19, it can be deduced that not all solutions are able to reach the maximum height increase: the K-braces + CLT core, indeed, fails to satisfy serviceability checks at $\Delta H = 12$ m, the X-braces + CLT core fails at $\Delta H = 20$ m and the V-braces + CLT core fails at $\Delta H = 28$ m. The braced tube + CLT core complies with the serviceability check at $\Delta H = 28$ m, thus allowing us to obtain a timber-only solution for a building of 96.20 m.

For the sake of brevity, hereafter, the characteristics and response parameters of the various structural options are presented and discussed only in step 3.

In Figure 20, the structural mass of the different solutions is depicted with the percentage variation in each model mass with respect to the project model; the mass of the original project is also provided as a reference. It is interesting to observe that all alternatives have almost the same mass and are lighter than the original project, even with the floors' addition, thanks to the removal of concrete floors as a preliminary step for height increase. The comparable structural mass of the four solutions is particularly important for the braced tube solution, which with the same mass as the other systems allows for a significant increase in stiffness, with a consequent enhancement of structural efficiency.

The comparison in terms of fundamental vibration periods is reported in Figure 21, also with the percentage variation in each variant with respect to the project model. For all cases, the periods are lower than the original project, despite the building height increase, due to the reduction in the mass and the increase in lateral stiffness. The tube variant is characterized by the lowest vibration periods with 1.22 s along X and 2.03 s along Y.

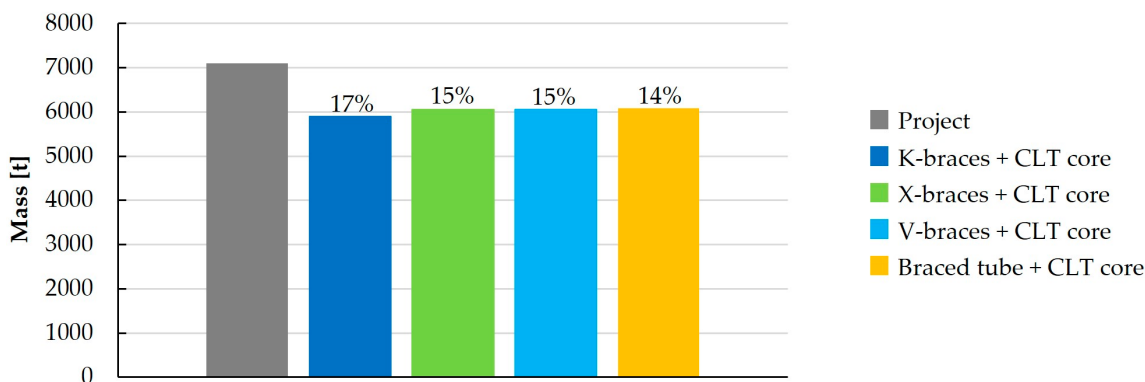


Figure 20. Total structural mass comparison—step 3.

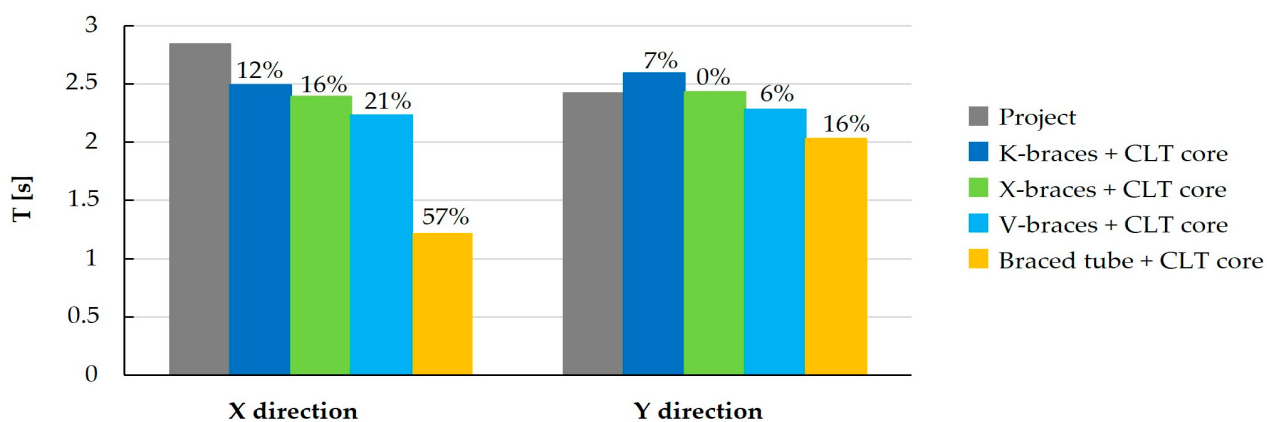


Figure 21. Vibrational periods comparison—step 3.

As anticipated, only the braced tube + CLT core satisfies the serviceability checks in the most critical direction (Y) in terms of top floor acceleration (Figure 22) and lateral displacements (Figure 23). In Figure 22, the percentage variation in the top floor acceleration of each variant with respect to the original project is also reported.

The percentage variation in the top floor displacement with respect to the limit of $H/500$ is equal to +41% for the K-braces + CLT core, +22% for the X-braces + CLT core, +8% for the V-braces + CLT core and −4% for the case of braced tube + CLT core.

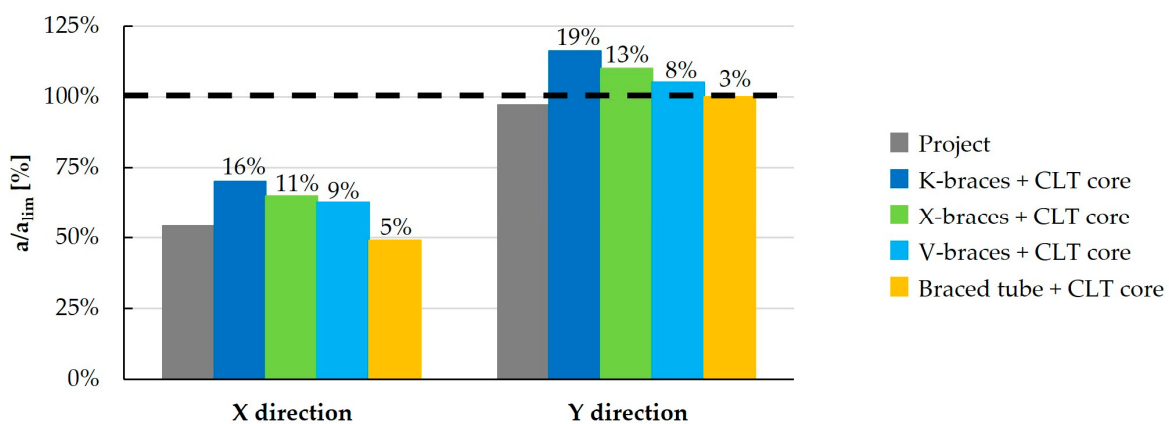


Figure 22. Top floor acceleration comparison—step 3.

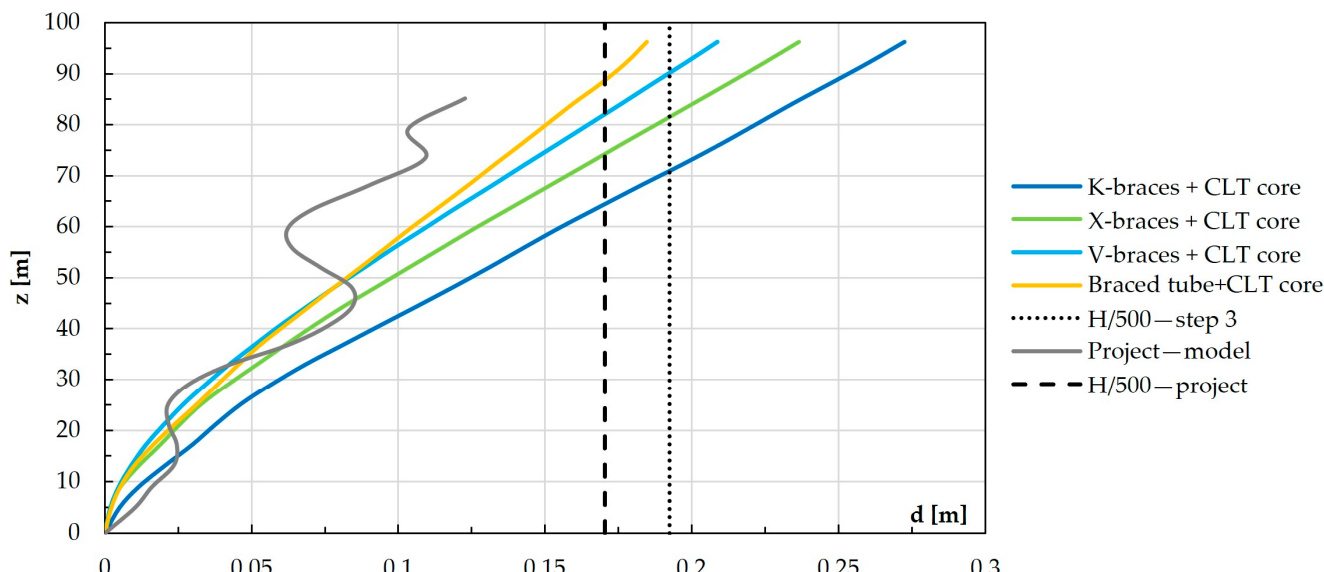


Figure 23. Absolute displacement comparison—step 3.

5.2.2. Hybrid Variants

The structural system that performs better is the braced tube. With this system, it is possible to increase the building height up to 96.2 m using only timber floors and timber structural elements. However, hybrid structural systems using steel or concrete to provide horizontal stability are nowadays widely adopted; therefore, two different steel–timber hybrid variants are studied considering the braced tube system. It is worth observing that the hybrid solutions are here considered not as a strategy to increase the building height but rather to develop a comparison in terms of sustainability with timber-only solutions, namely the one of the original project and the braced tube variant proposed.

For this reason, when defining hybrids, a stiffness-based equivalence criterion is adopted. Timber sections of members mainly subjected to axial deformations (columns and braces) are replaced with equivalent steel sections according to the following relationship:

$$[(E_t A_t)/L]_{\text{timber}} = [(E_s A_s)/L]_{\text{steel}}, \quad (2)$$

where:

- E_t is the elasticity module of timber;
- E_s is the elasticity module of steel.

Considering that the length L is the same, equivalent steel sections are derived as follows:

$$A_s = (E_t A_t)/E_s \quad (3)$$

In this way, the structural behavior under lateral loads (mainly governed by stiffness) of the hybrid structures should be approximately the same as the timber-only ones, and the two design approaches can be fairly compared in terms of sustainability. Quite trivially, given the ratio between the Young's moduli of steel and timber, the resulting steel cross-sections are quite a lot smaller than the timber ones.

Two different hybrid solutions are defined: one with steel braces only on the Y facades and another with steel braces on both the Y and X façades (Figure 24).

The behavior of these hybrid solutions and of the timber-only counterpart is almost the same, as can be seen in Figure 25 in terms of lateral displacements. Small differences arise due to the choice of available commercial sections for steel and to buckling checks.

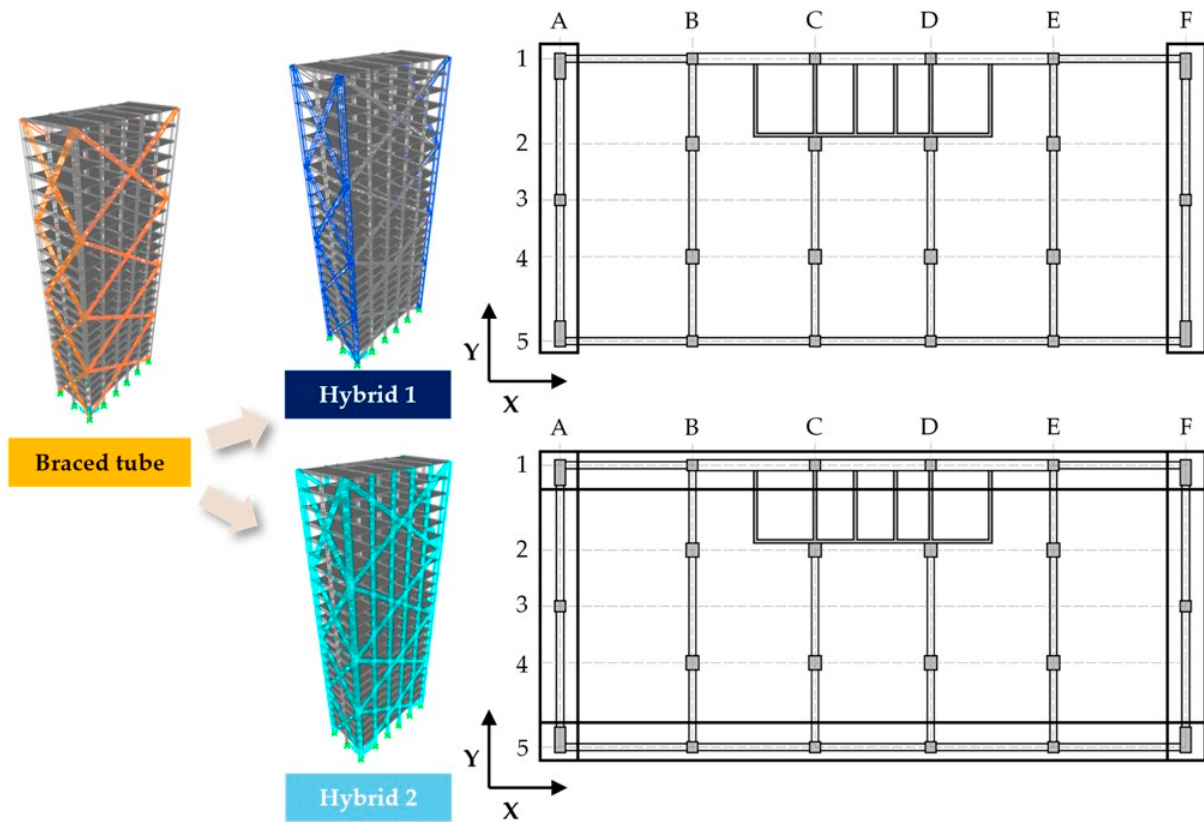


Figure 24. The two hybrid structures defined.

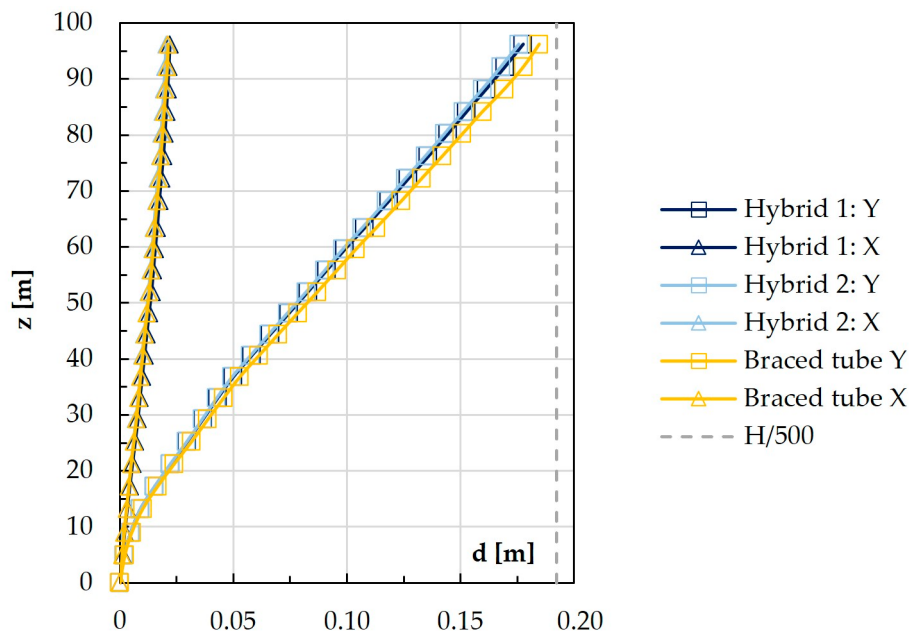


Figure 25. Lateral displacements—hybrid and timber-only braced tube solutions.

6. Sustainability

6.1. Life Cycle Assessment: General Aspects

The parameter used to define the sustainability of a proposal is related to the total GHG (greenhouse gas) emissions or removals associated with the whole life cycle, also called embodied carbon [35]. Embodied carbon is calculated considering different stages, as rep-

resented in Figure 26a, that, with reference to the Architecture–Engineering–Construction (AEC) industry, can be grouped into the following three stages.

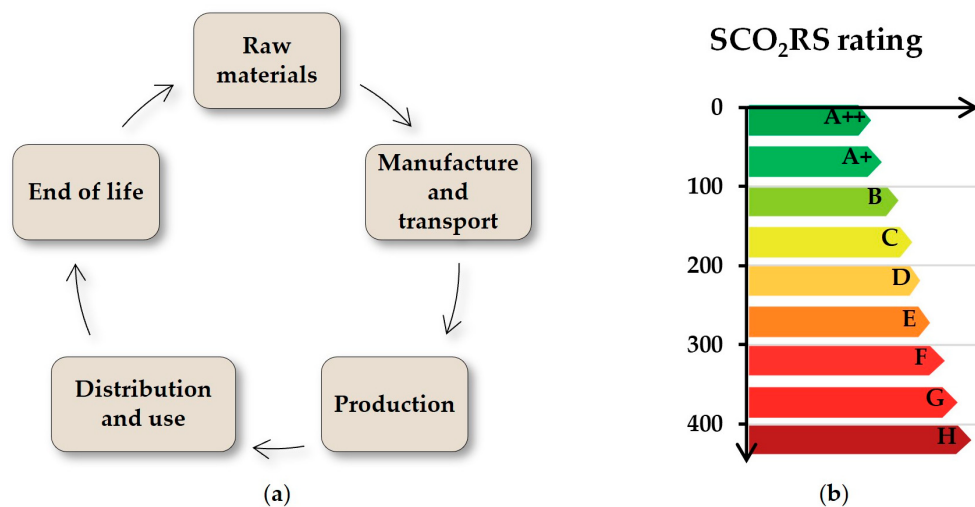


Figure 26. (a) LCA—life cycle assessment; (b) rating based on A1–A5 emissions, excluding sequestration or offsetting. Redrawn from [35].

1. Raw materials or product stage (cradle to gate): this stage considers the kgCO₂ released during the extraction, processing, manufacture and transportation of materials until products leave the factory gates to be taken to the site. The LCA parts that consider this stage are A1–A3.
2. Construction process stage: this stage considers kgCO₂ released during the transport of materials/products to the site, energy usage due to activities on site and kgCO₂ associated with the production, transportation and end-of-life processing of materials wasted on site. The LCA parts that consider this stage are A4 and A5.
3. End-of-life stage: this stage considers the kgCO₂ released during the demolition, deconstruction and transportation of materials away from the site and is considered in C1–C4.

There is also a module B, divided into modules B1 to B5, that considers embodied carbon associated with use, maintenance, replacements or change. This module is negligible when considering only structural components.

It is also possible to consider an additional module, called module D, that accounts for the benefits or loads beyond the project's life cycle, associated with recycling, energy production and reuse. Module D results are based on future scenarios for each material or component used in the project. The real impact of this module is very uncertain. The minimum LCA should include modules from A1 to A5. Generally, a carbon factor is defined as kgCO₂e/kg (e = equivalent) per unit of product; therefore, to calculate embodied carbon, the amount of each material should be multiplied by the relevant carbon factor for each life cycle module considered. Considering only modules from A1 to A5, it is possible to define a score based on the SCO₂RS classification reported in Figure 26b.

For steel products, the carbon factors vary depending on recycled content and production methods. A basic oxygen furnace (BOF) uses fossil fuels and a large quantity of virgin iron ore, while an electric arc furnace (EAF) is powered by electricity and produces steel with a high quantity of recycled content (up to 100%). Steel production with EAFs has a lower carbon factor than other production methods. Carbon factors also vary as a function of the specific steel product, e.g., closed sections have a carbon factor higher than open sections.

Wood is a highly appealing sustainable material since wood products require less energy to be produced than other materials. Also, wood sequesters carbon, as it is absorbed by the trees during growing, keeping it out of the atmosphere for the lifetime of the

building. This is called “biogenic carbon sequestration”; it can often balance the total embodied carbon impact of a building. Referring only to the structural components of a building, in Figure 27, the black upper line represents the total emissions related to the different life stages. These emissions are significant in the first stages (A1–A5) and in the last stages (C1–C4) but are negligible in stages B1–B7. The grey dotted line in Figure 27 represents the biogenic carbon sequestration that easily offsets the total embodied carbon emissions of the structure at least as long as the wood is kept inside the building.

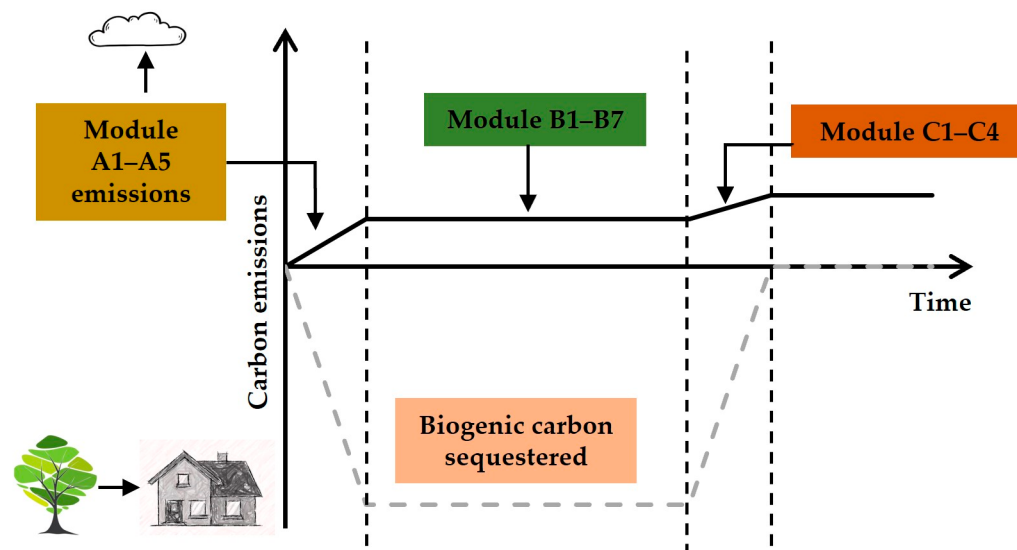


Figure 27. Carbon for timber structure. Remake from [35].

Clearly, if wood is reused at the end of the building's lifetime, this process will continue in time [35], providing a great benefit that lasts as long as the carbon is kept within the structure. LCA modules A1–A5 should not include biogenic carbon; instead, when a complete LCA is performed, biogenic carbon should be considered.

6.2. Life Cycle Assessment of the Case Study and Its Variants

Embodied carbon is calculated for the as-designed Mjøstårnet building, the taller timber-only braced tube variant (+7 floors, all timber, with a total height of 96.2 m) and the two structurally equivalent steel–timber hybrid solutions. For each model, the embodied carbon is first calculated considering modules A1–A5 only; afterward, the whole LCA (modules A–D) is considered, and the differences between the two approaches are evaluated. Carbon factors adopted for stages A1–A5 [35] are reported in Table 8, while in Table 9, the carbon factors adopted for stages C–D [35] are provided; finally, likely end-of-life scenarios for each material used [35] are reported in Table 10.

Table 8. Carbon factors adopted in stages A1–A5 for different materials and sections.

	A1–A3	A4	A5w
Timber frame	0.28	0.005	0.003
CLT panels	0.25	0.005	0.003
LVL floors	0.39	0.005	0.003
Concrete	0.175	0.0032	0.012
Steel rebar	0.196	0.0032	0.11
Steel closed sections	2.50	0.0032	0.0163
Steel open sections	1.50	0.0032	0.0163

Table 9. Carbon factors adopted in stages C and D for different materials and sections.

	C1	C2	C3–4	D
Timber	3.40	0.005	1.66	−0.524
Concrete	3.40	0.005	0.013	−0.001
Steel rebar	3.40	0.005	0.013	0.351
Steel profiles	3.40	0.005	0.013	−1.53

Table 10. End-of-life scenarios assumed.

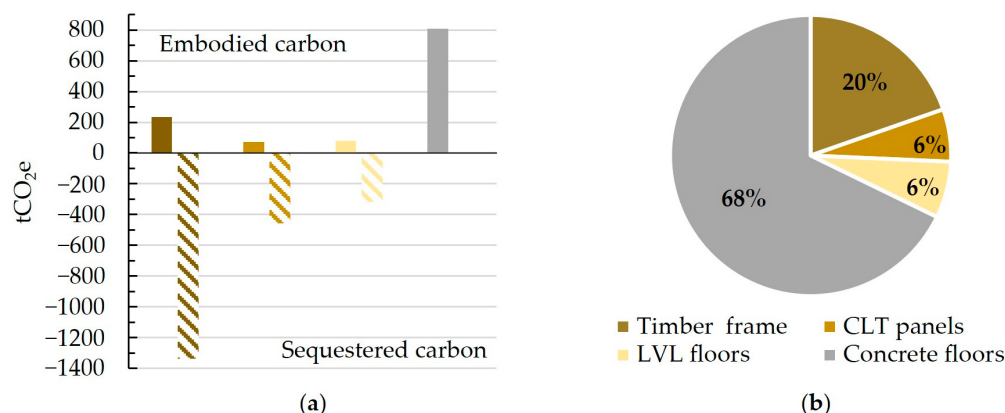
End-of-Life Scenarios	
Steel	97% recycling
Timber	44% incineration for energy recovery 1% landfill 0% reuse 55% recycling
Concrete	90% recycling as aggregate

The results obtained for the original project both considering the modules A1–A5 only and the whole LCA are reported in Table 11. The results obtained from A1–A5 and A–C are not very different from each other with a discrepancy equal to 9%. Clearly, with a full LCA, also considering module D, the building exhibits a better response in terms of embodied carbon.

Table 11. LCA results—original project.

	tCO _{2e}	tCO _{2e} /m ²
A1–A5	1193	132
Sequestered carbon	−2113.39	−234
A–C	1307	145
Module D	−641	−71

The results obtained for modules A1–A5 are reported in Figure 28. It can be observed that most of the embodied carbon is related to the concrete elements, while timber products only represent 32%. Referring to results obtained from modules A1–A5, it is also possible to classify the building in terms of embodied carbon per square meter: with the value of 132 tCO_{2e}/m², the original project falls in class B, as shown in Figure 29.

**Figure 28.** Original project: (a) embodied carbon A1–A5 and sequestered carbon; (b) percentage of total embodied carbon A1–A5 for each structural material.

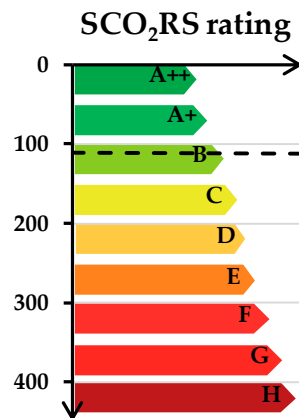


Figure 29. SCO₂RS rating for the original project.

The LCA results for the timber-only braced tube solution, with additional floors with respect to the original project, are reported in Table 12. These results suggest an improvement in the sustainability of the design despite the height increase. In particular, the results obtained for the modules A1–A5 are reported in Figure 30.

Table 12. LCA results—timber-only braced tube with additional floors.

	tCO _{2e}	tCO _{2e} /m ²
A1–A5	650	51
Sequestered carbon	-3465	-272
A–C	746	58
Module D	-1107	-87

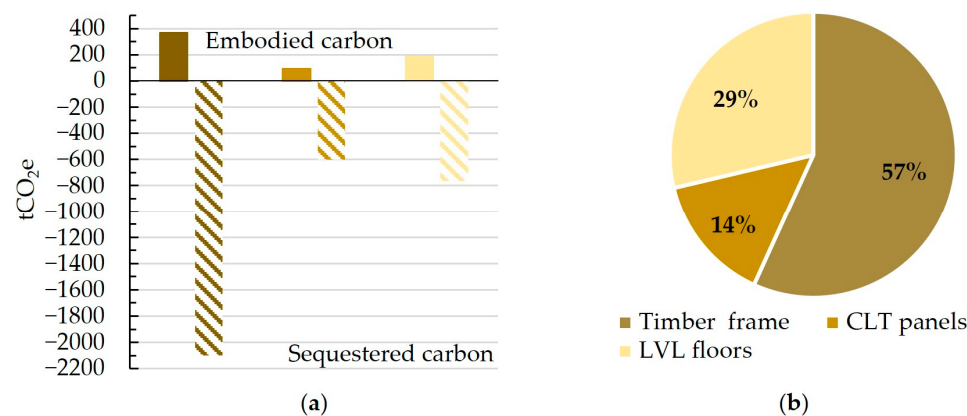


Figure 30. Timber-only braced tube with additional floors: (a) embodied carbon A1–A5 and sequestered carbon; (b) percentage of total embodied carbon A1–A5 for each structural material.

Referring to the results obtained from modules A1–A5, it is also possible to classify the building in terms of embodied carbon per square meter: with the value of 51 tCO_{2e}/m², the timber-only braced tube solution falls into class A+, as shown in Figure 31. Therefore, this solution, which represents the most efficient in terms of structural performance, is also the most sustainable one thanks to the low embodied carbon related to timber products.

The LCA results obtained for the hybrid timber–steel solutions 1 and 2 are, respectively, reported in Tables 13 and 14. The results are far away from those obtained in the previous case with a percentage increase, with respect to the original project, equal to 18–21% (modules A1–A5/A–C) for the first hybrid solution and 52–56% (modules A1–A5/A–C) for the second hybrid solution. Despite this, the use of steel products has a great positive

impact on the end of life of the structure considering the whole LCA with module D thanks to the recycling of steel products, as can be seen in Tables 13 and 14.

Today, in fact, as mentioned earlier, steel is amiably recycled with percentages higher than 90%, while wood is still mostly burned for energy production.

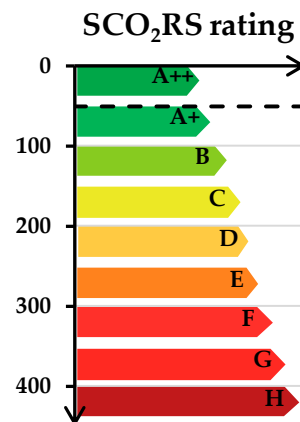


Figure 31. SCO₂RS rating for the timber-only braced tube with additional floors.

Table 13. LCA results—hybrid timber–steel braced tube solution 1, with additional floors.

	tCO ₂ e	tCO ₂ e/m ²
A1–A5	1501	118
Sequestered carbon	−2796	−219
A–C	1591	125
Module D	−1512	−118

Table 14. LCA results—hybrid timber–steel braced tube solution 2, with additional floors.

	tCO ₂ e	tCO ₂ e/m ²
A1–A5	2714	213
Sequestered carbon	−2253	−177
A–C	2730	214
Module D	−2186	−171

The results obtained for modules A1–A5 are reported in Figures 32 and 33.

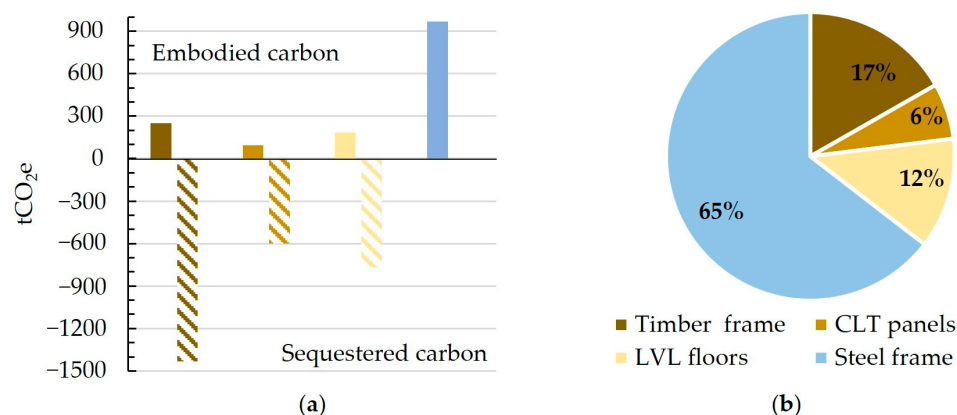


Figure 32. Hybrid timber–steel braced tube solution 1, with additional floors: (a) embodied carbon A1–A5 and sequestered carbon; (b) percentage of total embodied carbon A1–A5 for each structural material.

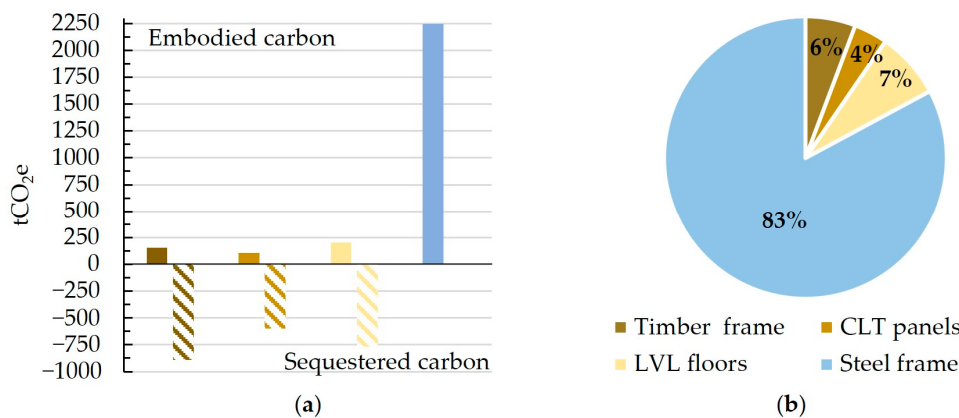


Figure 33. Hybrid timber–steel braced tube solution 2, with additional floors: (a) embodied carbon A1-A5 and sequestered carbon; (b) percentage of total embodied carbon A1-A5 for each structural material.

The results are clearly higher than those obtained in the other cases analyzed. The use of steel products has a negative impact on the first module of the LCA but has a great positive impact at the end of the life of the structure considering the whole LCA with module D.

Referring to results obtained from modules A1–A5, it is also possible to classify the two solutions in terms of embodied carbon per meter squared. While solution 1 falls into class B, solution 2 is in class D, as shown in Figure 34.

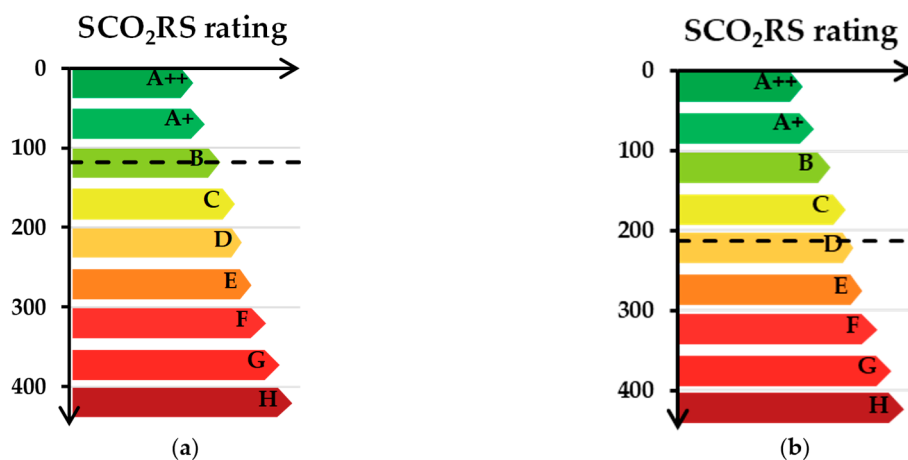


Figure 34. SCO₂RS rating for hybrid braced tube with additional floors: (a) solution 1, (b) solution 2.

A comparison between the four building solutions is provided in Figure 35, where the embodied carbon values at the different stages of the LCA are explicitly shown. For each solution, the analysis results obtained considering either modules A1–A5 or A–C are almost the same with a discrepancy equal to 9% for the project case, 15% for the braced tube, 6% for the first hybrid solution and 1% for the second hybrid solution. From this direct comparison, it clearly emerges that the timber-only braced tube is the best solution, better than the initial model even if seven additional floors are added, with a percentage reduction of embodied carbon equal to 43–46%. This depends on the greater quantity of wood used. The first hybrid solution presents results that are comparable to those of the original project with a percentage increment of embodied carbon equal to 18–21%, thus appearing as a competitive alternative, both from structural and sustainability points of view. The second hybrid solution, using a larger amount of steel material, presents the highest values of total equivalent embodied carbon with a percentage increment of 52–56% with respect to the original project model.

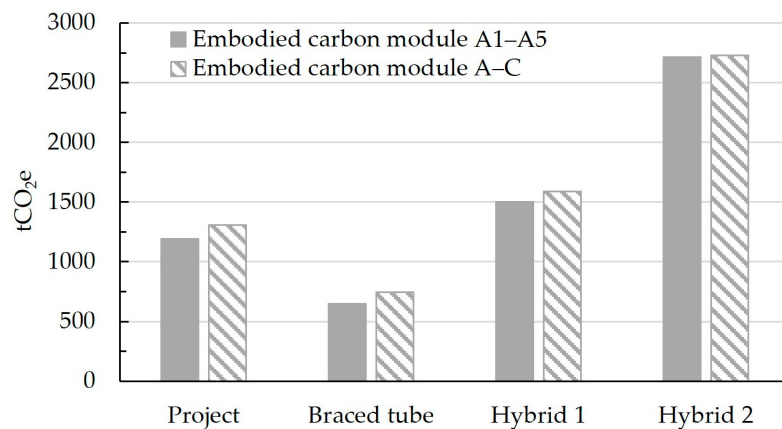


Figure 35. Comparison of the four solutions in terms of total embodied carbon.

In Figure 36, only the LCA results of modules A1–A5 are reported, along with the biogenic carbon sequestered. Biogenic carbon in the three alternative solutions is always greater than in the original project due to the greater amount of employed wood material. However, when considering only modules A1–A5, sequestered biogenic carbon cannot be considered but only reported separately.

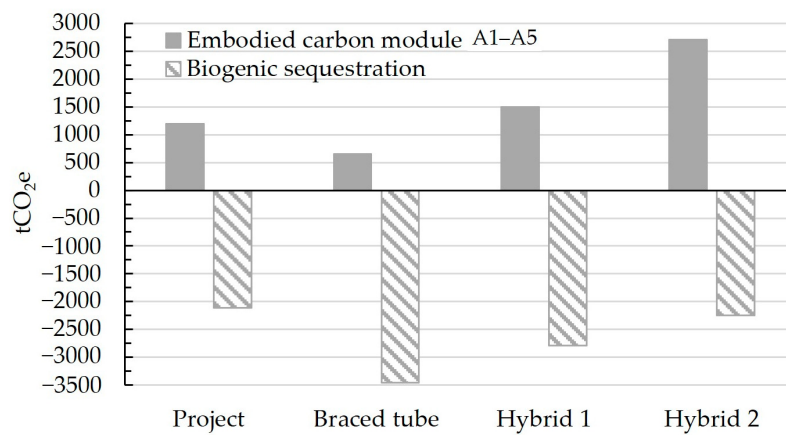


Figure 36. Comparison of the four solutions in terms of total embodied carbon modules A1–A5.

In Figure 37, the results related to modules A–D are reported.

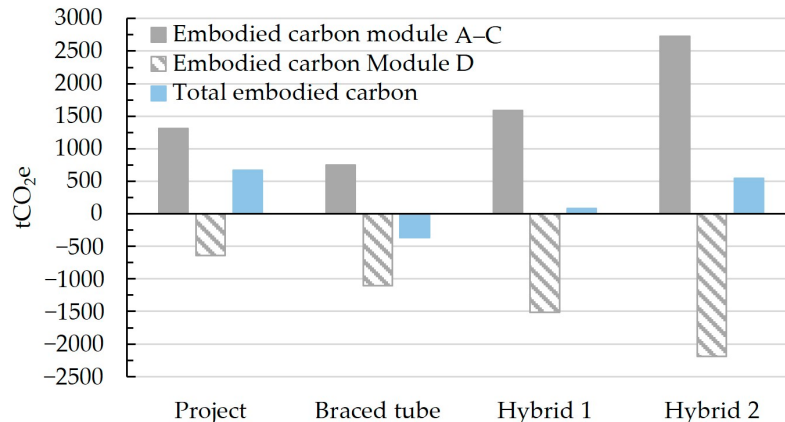


Figure 37. Comparison of the four solutions in terms of total embodied carbon modules A–C + D.

The first column provides the results obtained from modules A–C for each structural solution; therefore, it represents the total equivalent embodied carbon emitted. Clearly, using steel rather than wood increases the embodied carbon. The second column, with a negative quantity of equivalent embodied carbon, derives from module D and increases with the amount of steel due to the potential for recycling or reuse of steel products. The third column is given by the sum of the first and second columns, i.e., of results from modules A–C and D; therefore, the third column represents the results that would be obtained at the actual occurrence of the assumed end-of-life scenario. In such a case, the results obtained for the three variants here considered would always be better than for the original project thanks to the recycling potential of steel products and the great sustainability of timber elements. Therefore, hybrid solutions, which represent suitable design choices for rational structures of taller buildings, can also be highly sustainable solutions.

7. Conclusions

In this paper, alternative structural solutions to increase the height of the current tallest timber building in the world are explored and discussed in terms of structural performance and sustainability. For this purpose, a case study, the Mjøstårnet ($H = 85.4$ m), which is the tallest timber building worldwide, is assumed as an archetype for exploring design structural variants while increasing the building height. From the study here developed, it is possible to assert the following:

- Timber buildings are characterized by a low stiffness and light weight of structural members. The lightness of timber structures is unquestionably an advantage for both the design of the gravity load resisting system (including the foundation structure) and for the dramatic reduction in costs of construction (easiness of handling in the yard and fewer manpower) with consequent greater safety. Nevertheless, the flexibility that requires very large sections to comply with drift and acceleration limitations, combined with the lightness of timber structures, represents a serious problem in terms of serviceability assessments.
- Timber buildings require structural systems specific for very tall buildings at much lower heights than in the case of steel or concrete solutions. As a result of the design exploration, the most sustainable and efficient timber-only structural system is the braced tube, able to push the height of the building case study up to 96.2 m through the addition of seven extra floors. The tube solution appears more efficient than the original project, both in terms of structural performance and sustainability indexes. Alternative systems employing different braced bays (V- and X-braces) are not able to reach greater heights. In fact, it is necessary to earn the needed lateral stiffness by involving all perimeter structural elements, thus activating the three-dimensional (tube) behavior of the building.
- Timber–steel hybrid solutions, characterized by Glulam timber beams, columns and floors with a CLT core in combination with steel bracing systems, represent valid alternatives that define an optimal balance between structural behavior and sustainability to reach greater heights. Indeed, the use of braces made of steel, which are characterized by a much higher stiffness than timber, determines a greater lateral stiffness of the overall structures and, therefore, smaller members; further, the steel products also have good performance in terms of embodied carbon if the whole LCA is considered thanks to their potential for recycling and reuse.

Definitely, today, timber–steel hybrids represent very interesting structural solutions for designing efficient and sustainable high-rise buildings thanks to the combination of the mechanical properties of steel with the low carbon and lightness of wood.

Author Contributions: Conceptualization, F.A., F.E., G.I., D.F., B.F. and E.M.; methodology, F.A., F.E., G.I., D.F., B.F. and E.M.; software, F.A.; validation, F.A., F.E., G.I., D.F., B.F. and E.M.; formal analysis, F.A.; investigation, F.A., F.E., G.I., D.F., B.F. and E.M.; resources, F.A., F.E., G.I., D.F., B.F. and E.M.; data curation, F.A., F.E., G.I. and D.F.; writing—original draft preparation, F.A., F.E., G.I., D.F., B.F.

and E.M.; writing—review and editing, F.A., F.E., G.I., D.F., B.F. and E.M.; visualization, F.A., F.E., G.I., D.F., B.F. and E.M.; supervision, B.F. and E.M.; project administration, B.F. and E.M. All authors have read and agreed to the published version of the manuscript.

Funding: This research received no external funding.

Data Availability Statement: Data are contained within the article.

Acknowledgments: The research project DPC–ReLUIIS 2022–2024—WP13 Contribution to standards for timber structures is acknowledged.

Conflicts of Interest: The authors declare no conflicts of interest.

References

- Arnold, W. The structural engineer’s responsibility in this climate emergency. *Struct. Eng. J. Inst. Struct. Eng.* **2020**, *98*, 10–11. [[CrossRef](#)]
- Moynihan, M. Held to carbon account: The end of ‘bog standard’ new build? *Struct. Eng. J. Inst. Struct. Eng.* **2020**, *98*, 62–65. [[CrossRef](#)]
- United Nations Environment Programme. *Buildings and Climate Change: Summary for Decision Makers*; United Nations Environment Programme: Nairobi, Kenya, 2009.
- United Nation, Department of Economic and Social Affairs, Population Division. *World Population Prospects 2022: Summary of Results*; United Nation: New York, NY, USA, 2022.
- Al-Kodmany, K.; Du, P.; Ali, M.M. *Sustainable High-Rise Buildings: Design, Technology, and Innovation*, 1st ed.; The Institution of Engineering and Technology: London, UK, 2022; pp. 1–13.
- Dean, B.; Dulac, J.; Petrichenko, K.; Graham, P. Towards zero-emission efficient and resilient buildings. In *Global Status Report*; Global Alliance for Buildings and Construction: Paris, France, 2016.
- European Commission. *Roadmap to a Resource Efficient Europe*; COM/2011/0571 Final; European Commission: Brussels, Belgium, 2011.
- EC, Science for Environment Policy, Future brief: No net land take by 2050? 2016.
- Al-Kodmany, K.; Ali, M.M. *The Future of the City: Tall Buildings and Urban Design*, 1st ed.; WIT Press: Southampton, UK, 2013.
- Kuzmanovska, I.; Gasparri, E.; Monné, D.T.; Aitchison, M. Tall Timber Buildings: Emerging Trends and Typologies. In Proceedings of the World Conference on Timber Engineering, Seoul, Republic of Korea, 20–23 August 2018.
- Buchanan, A.H.; John, S.; Love, S. Life cycle assessment and carbon footprint of multi-story timber buildings compared with steel and concrete buildings. *N. Z. J. For.* **2013**, *57*, 9–18.
- Krötsch, S.; Müller, L. The Development of Multi-Storey Timber Construction. In *Manual of Multi-Storey Timber Construction*, 1st ed.; Kaufmann, H., Krötsch, S., Winter, S., Eds.; Detail Business Information GmbH: Munich, Germany, 2018; pp. 10–13.
- Svatoš-Ražnjević, H.; Orozco, L.; Menges, A. Advanced Timber Construction Industry: A Review of 350 Multi-Storey Timber Projects from 2000–2021. *Buildings* **2022**, *12*, 404. [[CrossRef](#)]
- Safarik, D.; Elbrecht, J.; Miranda, W. State of tall timber 2022. *CTBUH J.* **2022**, *2022*, 22–29.
- Karacabeyli, E.; Lum, C. *Technical Guide for the Design and Construction of Tall Wood Buildings in Canada*, 2nd ed.; Special Publication SP-55E; FPInnovations: Vancouver, BC, Canada, 2022.
- Smith, I.; Frangi, A. *Use of Timber in Tall Multi-Story Buildings, Structural Engineering Document 13*; International Association for Bridge and Structural Engineering (IABSE): Zurich, Switzerland, 2014.
- SOM. *Timber Tower Research Project, Final Report*; Skidmore, Owings and Merrill, LLP: Chicago, IL, USA, 2013.
- Connoly, T.; Loss, C.; Iqbal, A.; Tannert, T. Feasibility Study of Mass-Timber cores for the UBC Tall Wood Building. *Buildings* **2018**, *8*, 98. [[CrossRef](#)]
- Angelucci, G.; Mollaioli, F.; Molle, M.; Paris, S. Performance assessment of Timber High-rise Buildings: Structural and Technological Considerations. *Open Constr. Build. Technol. J.* **2022**, *16*, e187483682206270. [[CrossRef](#)]
- BCSA. *UK Structural Steelwork: 2050 Decarbonisation Roadmap*; The British Constructional Steelwork Association Limited: London, UK, 2021; pp. 6–7.
- Abrahmsen, R. Mjostarnet—Construction of an 81 m tall timber building. In Proceedings of the Internationales Holzbau forum IHF, Aus der Praxis—Für die Praxis Kongresszentrum-Garmisch-Partenkirchen, Innsbruck, Austria, 6–8 December 2017.
- Abrahmsen, R. Mjostarnet—18 storey timber building completed. In Proceedings of the Internationales Holzbau forum IHF, Kongresszentrum, Garmisch-Partenkirchen, Germany, 5–7 December 2018.
- Tulebekova, S.; Malo, K.A.; Rønnquist, A.; Nåvik, P. Modeling stiffness of connections and non-structural elements for dynamic response of taller glulam timber frame buildings. *Eng. Struct.* **2022**, *261*, 114209. [[CrossRef](#)]
- Metsä. Available online: <https://www.metsagroup.com/metsawood/explore-wood/kerto-lvl-applications/floor-elements/> (accessed on 14 December 2023).
- Finnish Woodworking Industries. *LVL Handbook Europe*; Federation of the Finnish Woodworking Industries: Helsinki, Finland, 2019; pp. 50–107.
- Hon, K.C. Two-way coupled fluid-structure interaction method on aerodynamic analysis of tall timber building using URANS. Master’s Thesis, Oslo Metropolitan University, Oslo, Norway, 6 June 2021.

27. Youtube. Available online: <https://www.youtube.com/watch?v=yIBXyMQu1DE&t=40s> (accessed on 14 December 2023).
28. Sweco. Available online: <https://www.sweco.dk/en/showroom/mjoestaarnet/> (accessed on 14 December 2023).
29. EN 1991-1-4:2005; Eurocode 1—Actions on Structures—Part 1–4: General Actions—Wind Actions. European Committee for Standardization (CEN): Brussels, Belgium, 2004.
30. Computers and Structures, Inc. SAP2000 Linear and Nonlinear Static and Dynamic Analysis and Design of Three-Dimensional Structures; Computers and Structures, Inc.: Walnut Creek, CA, USA, 2009.
31. EN 14080: 2013; Timber structures—Glued Laminated Timber and Glued Solid Timber—Requirements. European Committee for Standardization (CEN): Brussels, Belgium, 2013.
32. EN 338: 2016; Structural timber—Strength Classes. European Committee for Standardization (CEN): Brussels, Belgium, 2016.
33. Magne, A.; (Sweco, Lillerhammer, Oppland, Norway, Europe). Personal communication, 2023.
34. ISO 10137:2007; Bases for Design of Structures—Serviceability of Buildings and Walkways Against Vibrations. International Organization for Standardization (ISO): Geneva, Switzerland, 2007.
35. Gibbons, O.P.; Orr, J.J.; Archer-jones, C.; Arnold, W.; Green, D. *How to Calculate Embodied Carbon*, 2nd ed.; The Institution of Structural Engineers: London, UK, 2022.

Disclaimer/Publisher's Note: The statements, opinions and data contained in all publications are solely those of the individual author(s) and contributor(s) and not of MDPI and/or the editor(s). MDPI and/or the editor(s) disclaim responsibility for any injury to people or property resulting from any ideas, methods, instructions or products referred to in the content.